Selectivity of dopamine D_1 and D_2 receptor agonists – A combined computational approach

Marcus Malo

UNIVERSITY OF GOTHENBURG

Department of Chemistry and Molecular Biology
University of Gothenburg
2012

DOCTORAL THESIS

Submitted for partial fulfillment of the requirements for the degree of
Doctor of Philosophy in Chemistry

Selectivity of dopamine D_1 and D_2 receptor agonists – A combined computational approach

Marcus Malo

Cover picture: The generated D_1 (yellow) and D_2 (blue) receptor models together with the selective D_1 (doxanthrine) and D_2 (*R*-NPA) agonists.

ISBN: 978-91-628-8572-4
http://hdl.handle.net/2077/30460

Department of Chemistry and Molecular Biology
University of Gothenburg
SE-412 96 Göteborg
Sweden

Printed by Ineko AB
Kållered, 2012

To my family

Abstract

Dopamine (DA) is an endogenous neurotransmitter acting in the central nervous system. DA plays a key role in many vital brain functions such as behavior, cognition, motor activity, learning, and reward. Dopamine receptors belong to the rhodopsin like family of G-protein coupled receptors (GPCRs). There are five subtypes of DA receptors (D_1-D_5), which are further divided into two main families based on sequence similarities and their coupling to intracellular signaling (D_1- and D_2-like receptors). Dopamine agonists mimic the effects of the natural neurotransmitter and it has been found that selective dopamine D_2 or D_1 and mixed D_1/D_2 agonists are useful in the treatment of Parkinson disease. As D_2 (but not D_1) agonists have shown undesirable dyskinetic effects it is of highest interest to understand the reasons behind D_1/D_2 agonist selectivity.

This thesis is focused on the identification of structural features that determine the selectivity of D_1 and D_2 receptor agonists for their respective receptors. Selective pharmacophore models were developed for both receptors. The models were built by using projected pharmacophoric features that represent the main agonist interaction sites in the receptor, and excluded volumes where no heavy atoms are permitted. The sets of D_1 and D_2 ligands used for modeling were carefully selected from published sources and consist of structurally diverse, conformationally rigid full agonists as active ligands together with structurally related inactives.

3D receptor models in their agonist bound state were also generated for dopamine D_1 and D_2, in order to get improved insight into agonist binding. The constructed D_1 and D_2 agonist pharmacophore models were superimposed into their corresponding receptor model. The arrangement of pharmacophoric features were in agreement with the position of the agonist key interacting amino acids in the binding site, with exception of one hydrogen bond accepting/donating feature in the D_2 model and the positioning of the excluded volumes in both models. Both pharmacophore models were refined to better reflect the shape of the binding pocket and had similar pharmacophore hit rate when screening the test sets of dopamine ligands. Several key factors for D_1/D_2 agonist selectivity were identified.

In addition, a semi-empirical method to model transmembrane proteins with focus on the ligand binding site has been developed. The method was evaluated by generating a β_1-adrenergic receptor model which had an RMSD of 1.6 Å for all heavy atoms in the binding site relative the crystal structure. A D_2 receptor model with an agonist present was constructed, but this model was unable to discriminate actives from inactives in a docking study.

Keywords: dopamine, agonists, GPCRs, pharmacophore modeling, protein structure modeling, agonist selectivity

Papers included in this thesis

This thesis is based on the following publications and manuscript, which will be referred to in the summary by their Roman numerals.

I. **Selective pharmacophore models of dopamine D_1 and D_2 full agonists based on extended pharmacophore features.**
Malo M., Brive L, Luthman K., Svensson P
ChemMedChem. **2010**, *5* (2), 232-46.

II, **Investigation of D_2 receptor-agonist interactions using a combination of pharmacophore and receptor homology modeling.**
Malo M., Brive L., Luthman K., Svensson P.
ChemMedChem **2012**, *7* (3), 471-82.

III. **Investigation of D_1 receptor-agonist interactions and D_1/D_2 agonist selectivity using a combination of pharmacophore and receptor homology modeling.**
Malo M., Brive L., Luthman K., Svensson P.
ChemMedChem **2012**, *7* (3), 483-494.

IV. **Development of 7TM receptor-ligand complex models using ligand-biased, semi-empirical helix-bundle repacking in torsion space: Application to the agonist interaction of the human dopamine D_2 receptor.**
Malo M.,* Persson R.,* Svensson P., Luthman K., Brive L.
Manuscript

* Equally contributing authors.

Contributions to the Papers

I. Formulated the research problem; performed all experimental work; interpreted the results, and wrote the manuscript

II. Formulated the research problem; performed most of the experimental work; interpreted the results, and wrote the manuscript

III. Formulated the research problem; performed most of the experimental work; interpreted the results, and wrote the manuscript

IV. Contributed to the outline of the study. Contributed to the interpretations of the results

Contents

Abbreviations

3D	Three dimensional
5-HT	5-Hydroxytryptamine (serotonin)
adr	Adrenergic receptor
DA	Dopamine
DHX	Dihydrexidine
DPAT	Dipropylaminotetralin
CNS	Central nervous system
drd	Dopamine receptor
EC	Extracellular loop
ΔG	Change in Gibbs free energy
ΔH	Change in enthalpy
ΔS	Change in entropy
GPCR	G-protein coupled receptor
IA	Intrinsic activity
IC	Intracellular loop
ICM	Internal coordinate mechanics
K_i	Inhibition constant
V_{LJ}	The Lennard-Jones potential
MC	Monte Carlo
MD	Molecular Dynamics
MM	Molecular Mechanics
MMFF	Merck Molecular Force Field
MOE	Molecular operating environment
NPA	*N*-Propyl-norapomorphine
PD	Parkinson´s disease
PES	Potential Energy Surface
PHNO	*N*-propyl-9-hydroxynaphthoxazine
OPLS	Optimized Potentials for Liquid Simulations
RMSD	Root-mean-square deviation
TM	Transmembrane α-helix
QM	Quantum Mechanical
QSAR	Quantitative structure-activity relationship

1. General introduction and aims of the thesis

Computational methods are widely used in drug discovery and development in both industrial and academic environments. How ligands interact with their biological targets can be studied in detail using different modeling approaches and these methods are often complementing each other. A combination of methods is in many cases necessary as the information regarding structural characteristics and mechanistic properties of both targets and ligands may be limited. Validation with experimental work provides an improved possibility to interpret the experimental data and also provide ideas for new strategies.

If ligands with a desirable pharmacological profile are known, ligand-based approaches such as quantitative structure-activity relationships (QSARs) and pharmacophore modeling can be applied. These methods are used to collect common structural features from the ligands in order to provide knowledge regarding ligand/protein interaction, target selectivity and ligand affinity.

Even if the target structure including the binding site is known it may be a difficult task to predict how a given ligand binds. Docking programs are used to predict protein bound ligand poses in a predefined binding pocket and each binding mode can be ranked with respect to scoring functions.[1] Structural information of biological macromolecules is available in the Protein Data Bank (PDB),[2] but the detailed structures of several drug relevant targets are still unknown. Modeling techniques such as homology modeling can be used to predict 3D-structures if the structure of a related protein has been determined.[3]

Dopamine (DA) receptors in the central nervous system (CNS) play a major role in the initiation and control of many vital brain functions such as behavior, cognition, motor activity, learning, and reward.[4] There are five types DA receptors which are further divided into two main families D_1- (D_1 and D_5) and D_2-like ($D_{2\text{-}4}$). Detailed knowledge regarding subtype-selective agonists will improve the understanding of the role of D_1- and D_2-like receptor signaling in normal CNS function as well as in disease. The work

presented in this thesis deals both with structure and ligand based modeling strategies and the overall aim of the thesis is to investigate the reasons behind dopamine D_1 and D_2 receptor agonist selectivities using both pharmacophore and homology modeling and combinations thereof.

This has been achieved by

- generating D_1 and D_2 agonist pharmacophore models based on sets of carefully selected active and inactive ligands
- using a combined pharmacophore and receptor modeling approach to identify factors determining the agonist selectivity for both the D_1 and D_2 receptors
- comparing the D_1 and D_2 agonist models to extract the factors determining the D_1/D_2 agonist selectivity

Another aim was to develop a novel GPCR modeling method, based on repacking of the bundle of transmembrane helices of a receptor homology model having a ligand present in the binding site during the procedure.

2. Background

2.1. Proteins as drug targets

Most drugs act by binding to a target and affect its function in some way. The targets are in most cases proteins and are commonly divided into four categories:

- *Enzymes* – proteins catalyzing a chemical conversion of a substrate to a product. Enzymes are selective for their substrate and speed up the reaction rate by lowering the energy barrier for the biochemical reaction.
- *Carrier proteins* – cell membrane bound proteins actively transporting ions, small molecules or other substrates across membranes. The substrate binds to the carrier protein from one side of the membrane, this causes a translocation and the protein opens up on the other side. The substrate is released as the binding affinity decreases.
- *Ion channels* – membrane proteins gated by different mechanisms, for example by ligand binding or by transmembrane voltage changes. The role of ion channels is mainly to regulate biological processes involved in rapid changes, such as in muscle cells during a muscle contraction.
- *Receptors* – proteins located within the cell membrane, at the surface of the cell membrane or in the cytoplasm. A molecule, e.g. a hormone or a transmitter binds to the receptor and triggers a conformational change of the ligand-receptor complex which further leads to a biological response.

G-protein coupled receptors (GPCRs) followed by ion channels and nuclear receptors are the most common targets for drugs available on the market today.[5]

2.2. Protein structure

To be able to study how drugs interact with their targets a good understanding of the protein structure and function is required. Proteins consist of chains of amino acids and the twenty naturally occurring amino acids have different physicochemical properties. The

physicochemical characteristics of the amino acids (i.e. acidic or basic, hydrophilic or hydrophobic properties) determine their capability to participate in different types of binding interactions. The amino acids are linked together with amide bonds, often referred to as peptide bonds, and the chain folds into specific 3D protein structures. Protein structures are classified in four levels:

- primary – the order in which the individual amino acids are linked in the peptide chain (protein sequence)
- secondary – there are two main secondary structures, α-helices and β-sheets, both described by Pauling in 1951,[6-7] that are defined by the patterns of hydrogen bonds between the amide bonds in the protein backbone
- tertiary – the overall 3D shape of a subunit in a protein consisting of folded α-helices and β-sheets connected by turns and loops
- quaternary – arrangement of multiple subunits that can be identical (homomeric) or different (heteromeric)

2.3. Protein/ligand interactions

The most common types of interactions between the protein and the ligand are ionic interactions, hydrogen bonding and different hydrophobic interactions (**Figure 1**). In addition, interactions involving metal ions can be relevant for the stabilization of ligand/protein complexes or be important for protein function.[8] The energy of binding of the ligand is mostly governed by intermolecular van der Waals attractive forces, hydrogen bonding interactions, and repulsive forces like the hydrophobic effect that drives a molecule from the aqueous environment into the more hydrophobic cavity of a protein. The strength of the protein/ligand interaction is given by the inhibition constant, K_i, from which the binding energy, ΔG, can be calculated (*Eq* 1).

$$\Delta G = RT \cdot lnK_i = \Delta H - T\Delta S \quad (Eq\ 1)$$

Thus, both enthalpy (Δ*H*) and entropy (Δ*S*) contribute to the binding affinity. The entropy increases e.g. by introduction of larger more lipophilic substituents in the ligand, by decreasing the conformational degrees of freedom in the ligand or by displacement of

ordered water molecules.[9] Enthalpy can be optimized by establishing hydrogen bonds and vdW interactions, however considerations on how to optimize geometries are then required. For example, van der Waals interactions are maximized by an optimal geometric fit between drug and target, while the strength of hydrogen bonds is maximal when the distance and angle between acceptors and donors are optimal. In addition, an unfavorable enthalpy can be associated with the desolvation of polar groups.[9]

2.3.1. Ionic interactions

The ionic interaction is an electrostatic attraction between two oppositely charged ions, an anion and a cation. A pure ionic bond does not exist, since the bond always contains some degree of covalent bonding. The bond length is the sum of the radii of the two ions and the strength of the bond depends on the difference in electronegativity. The potential energy is a result of the strength F which is determined by Coulomb's law (*Eq2*), where the force F is directly proportional to the product of the point charges (q_1 and q_2) of the ions and inversely proportional to the square distance between the ions (r^2). k_e is Coulomb's constant (**Figure 1**).

$$F = k_e \frac{|q_1 \cdot q_2|}{r^2} \quad (Eq2)$$

2.3.2. Hydrogen bonds

Pauling stated in 1960[10] that a hydrogen bond is formed between X-H and Y, where X and Y are O and/or N (**Figure 1**), however the concept of hydrogen bonding was mentioned already in 1912 by Moore and Windmill.[11] The most recent IUPAC definition of hydrogen bonds was published in 2011.[12] The bonds may occur between different parts of a single molecule (*intramolecular*), or as in the case of a protein/ligand interaction, between different molecules (*intermolecular*). The strength of the classical hydrogen bond differs considerably dependent on distance, angle, atoms involved and the environment, but in organic and biochemical systems they are considered to be within the range 3-7 kcal·mol^{-1}.[12-13] The hydrogen bond length between the heavy atoms in two water molecules is approximately 2.8 Å, and the optimal bond angle is 180 degrees (O···H-O). However, Baker and Hubbard[14] suggested that a hydrogen bond angle could not be smaller than 120 degrees and the distance between the heavy atoms ≤ 3.5 Å. The

contribution to the binding energy originates mainly from Coulombic forces, but the bond also has a covalent nature.[12]

Hydrogen bonds can be stabilized by ionic interactions, such interactions are stronger than neutral hydrogen bonds and are called charge (or ion) assisted hydrogen bonds.[12] In the case of a positively charged amino group and a negatively charged carboxylic acid oxygen ($[N\cdots H\cdots O]^{\pm}$) the optimal distance between the heavy atoms is approximately 2.5 Å, and the binding energy ca 15 kcal·mol^{-1}.[15]

Hydrogen bonds can also be formed between weak acids (e.g. C-H) and lone pair electrons (e.g. on O or N) as well as between weak acids and π-systems (e.g. C-H···π, or X-H···π [X = O or N]). These are weaker than classical hydrogen bonds (1-4 kcal·mol^{-1}), but are still considered important for ligand binding.[12-13, 16]

2.3.3. van der Waals interactions

A van der Waals interaction is the sum of the attractive or repulsive forces between dipoles and/or induced dipoles, between molecules or within a molecule (**Figure 1**). The Lennard-Jones potential (V_{LJ}) is often used as an approximation of the van der Waals forces as a function of distance (*Eq 3*) and the strength is typically 0.5-1 kcal·mol^{-1} per atom pair, e.g. between ligand and receptor. The term r_m is the distance when the potential reaches its minimum, at r_m the potential function has the value $-\varepsilon$ and r is the actual distance.

$$V_{LJ} = \varepsilon \left(\frac{r_m}{r}\right)^{12} - 2\left(\frac{r_m}{r}\right)^{6} \quad (Eq\ 3)$$

2.3.4. π-interactions

Aromatic systems are conjugated planar ring systems with delocalized π-electrons. They are dipoles with an electron-rich part around the π-system and a positive counterbalancing part, positioned on the hydrogen atoms. Two aromatic systems may interact with the rings perpendicular to each other (T-shaped or face to edge) or in a parallel displacement of the rings (**Figure 1**). Marsili et al.[17] have studied π-interactions between aromatic residues in protein structures and the relative positioning between their aromatic planes. They defined orientations of the ring with angles (ω, θ) and a distance (*r)* and found that the T-shaped configuration should have $4.5 < r < 5.5$ Å, $75^{\circ} < \theta < 90^{\circ}$ and $\omega < 15^{\circ}$, and

the parallel displacement configuration 3.5 < r < 4.5 Å, θ < 15º and ω < 30º (**Figure 2**). The free energy for the bond in the parallel displacement configuration is in the range of 1.3-2.3 kcal·mol^{-1} while it is 0.8-1.8 kcal·mol^{-1} for the T-shape configuration. The energies depend on the combination of residues, for example, in case of His-His interactions the parallel displacement configuration is highly favored (ΔE=1.6 kcal·mol^{-1}), while the T-shaped is found to be more stable in a Phe-Phe complex (ΔE=0.2 kcal·mol^{-1}).[17] The three different configurations, parallel displacement, T-shape and face-to-edge are almost isoenergetic, but the T-shape is considered as the global minimum for benzene dimers.[18]

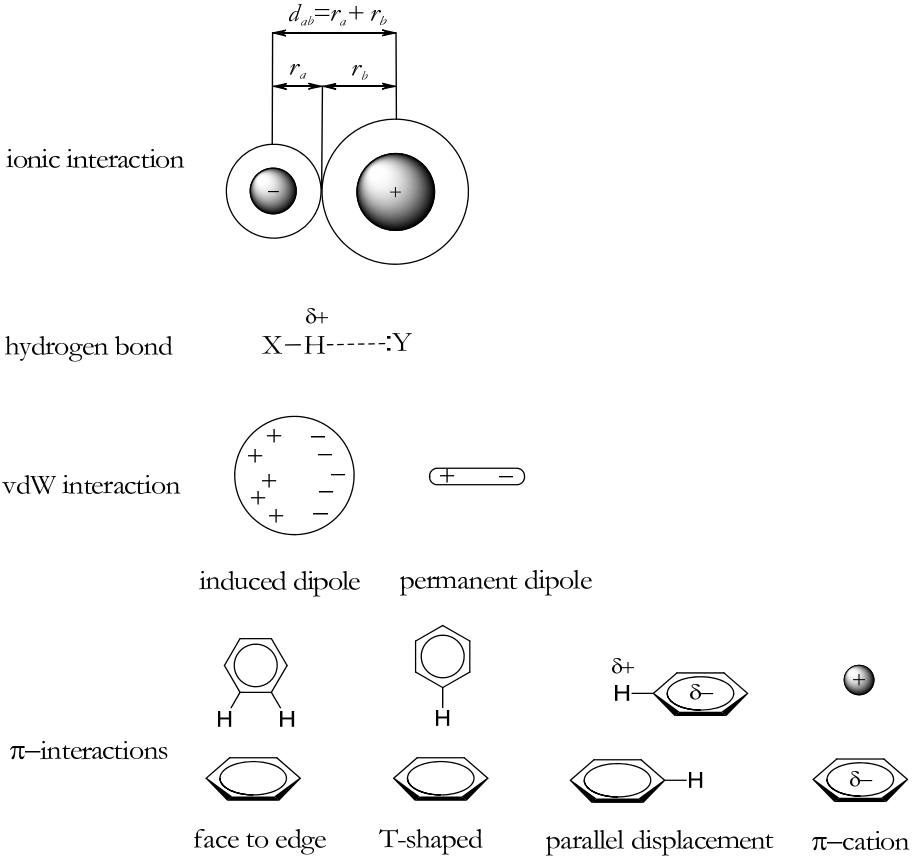

Figure 1. Important non-covalent protein/ligand interactions: i) ionic interactions, for which the bond length is defined as the sum of the ionic radii, d_{ab}, ii) hydrogen bonds, where the hydrogen is covalently bound to an electronegative donor (X) and further interacts with lone pair electrons of an electronegative acceptor (Y), iii) van der Waals interactions between an induced dipole and a permanent dipole, iv) π-interactions.

The delocalized electrons may also interact with cations, such as the interactions between aromatic residues in proteins and basic amino groups in ligands (**Figure 1**). These different π-interactions are essential and common contributors to binding in biological systems such as protein/ligand complexes.[17]

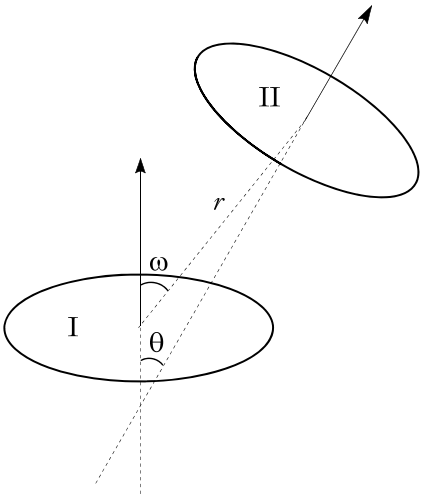

Figure 2. Coordinates defining the orientation of two planar moieties, I and II, e.g. two aromatic rings. θ defines the angle between the normals of each plane and ω defines the angle between the normal of ring I and the vector *r,* which connect the centroids of I and II.

2.4. Receptor agonists, antagonists, and inverse agonists

A ligand that binds to a receptor and triggers a physiological response is called an agonist for that receptor. Agonist binding can be characterized both in terms of how strong physiological response it triggers (intrinsic activity or efficacy) and of the concentration required to produce the response (affinity). High-affinity ligand binding indicates that a relatively low concentration of the ligand is needed to produce maximal physiological response, while low-affinity binding requires a higher relative concentration of the ligand. If a ligand triggers maximal intrinsic activity, it is defined as a *full agonist* (**Figure 3**). An agonist that can only partially activate the physiological response is called a *partial agonist*. Ligands that bind but fail to activate the receptor are *antagonists* whereas *inverse agonists* are ligands counteracts the activation by stabilizing the ground state of the receptor.[19] In some cases a ligand can produce a higher intrinsic activity than the full agonist and these ligands are referred to as *super agonists*.

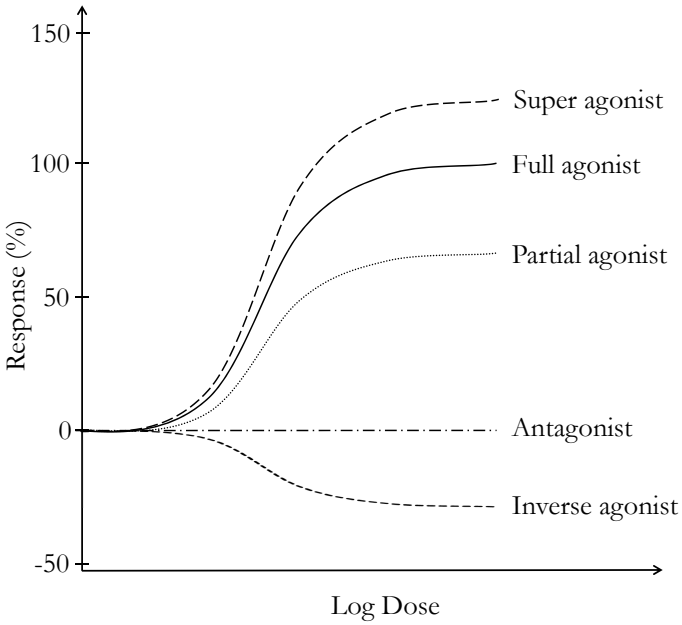

Figure 3. Dose-response curve illustrating super (long dash), full (solid), partial (dot) and inverse agonists (dash) together with a neutral antagonist (dash-dot).

2.5 G-protein coupled receptors (GPCRs)

2.5.1. GPCRs structure, function and activation

G-protein coupled receptors (GPCRs) are membrane proteins with seven transmembrane helices (TM1-7) which are connected by three intracellular (IC1-3) and three extracellular (EC1-3) loops (**Figure 4**).[20] GPCRs are divided into three main classes (A, B and C) where the Class A (the rhodopsin like superfamily) is the largest and accounts for over 80% of all GPCRs.[21] These receptors are involved in second messenger cascades via the guanine binding proteins (G-proteins). The domains that couple to G-proteins are expected to reside at the intracellular side, primarily the third intracellular loop (IC3). This conclusion has been supported by experiments performed to analyze the properties of GPCRs by deletion and replacement of the IC3 and site-directed mutation studies of particular amino acids in this loop.[20, 22-23]

The cytosolic signaling of GPCRs is catalyzed by endogenous agonists (such as neurotransmitters, hormones and autacoids) or synthesized analogs.[24-30] The agonist binding site in Class A GPCRs, is located in a cavity between the TM-helices at the

extracellular side and the binding of an agonist induces a movement of the helices at the cytoplasmic side. This has been shown by site-selective fluorescence labeling studies in which the magnitude of the fluorescence change was correlated with the agonist intrinsic activity.[25] These results indicate that there are numerous active conformations for a single receptor, and its ability to couple to the G-protein is dependent of the efficacy of the agonist. Kjelsberg et al.[22] have shown that mutations of an alanine residue close to the *C*-terminus of IC3 in the adrenergic α_{1b}-receptor with any of the 19 naturally occurring amino acids lead to various degrees of constitutive activation. The mutated receptors demonstrated higher affinity for agonists and even in absence of agonists the receptor mimicked an "active" state conformation. This indicates that the *C*-terminus of IC3 restricts the G protein coupling to the receptor, a constraint which is normally relieved by agonist occupancy.[22]

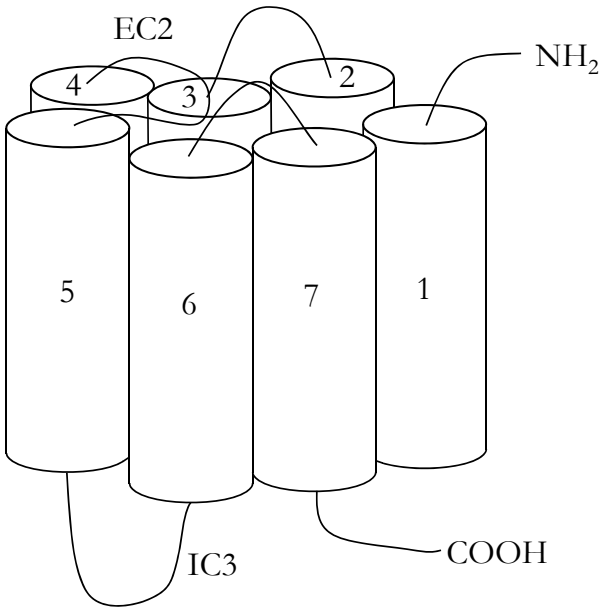

Figure 4. A schematic representation of a G-protein coupled receptor (GPCR). The peptide chain spans the membrane seven times and the transmembrane helices (TM 1-7) are annotated as cylinders. The *N*-terminus (NH_2) is located at the extracellular side, while the *C*-terminus (COOH) is located intracellularly. The membrane spanning regions are linked by three extracellular loops (EC) that alternate with three intracellular loops (IC). EC2 between TM4 and TM5 lines the binding crevice and are in many GPCRs involved in ligand binding. The G-protein couples to the IC3.

The subsequent signaling pathway depends on the type of G-protein that couples to the receptor. In some cases a single receptor is able to couple to several G-proteins and some receptors may also couple to β-arrestin, which in turn gives rise to completely different physiological responses.[31] These alternate signaling pathways are often referred to as *functional selectivity*.[32-33] The diversity of responses is based on the GPCR conformation, which can be ligand specific, i.e. ligands may stabilize different conformations of the receptor and thereby activate different signaling pathways.[34] This is often referred to as biased ligands.[32] Therefore functional selectivity is of high interest in the drug development process, but should not be confused with ligand selectivity.

Sodium ions have a negative modulatory effect on the agonist binding for several GPCRs including e.g. the A_{2A} adenosine[35] the α_2-adrenergic (adra2),[36] the dopamine D_1 (drd1)[37] and D_2 receptors (drd2).[38-39] In addition, the activation of the β_2 adrenoceptor[40] (adrb2) and the dopamine receptor has also been shown to be regulated by pH.[40-41] It has been suggested that the D(E)RY tripeptide sequence, the most conserved motif in Class A GPCRs which is located at the intracellular side of TM3, is important for receptor activation. Site-directed mutagenesis studies on the adra1b[42] and adrb2[40, 43] have shown that an ionic interaction between the most conserved residue, $Arg^{3.50}$† (in the DRY-motif) and the $Glu^{6.30}$ residue in TM6 restrains the movement of TM6 and stabilizes the inactive state of the receptor. A protonation of $Asp^{3.49}$ induces a conformational change of $Arg^{3.50}$ and the ionic lock is disrupted.[43] That means that at lower pH the receptor state equilibrium will be shifted towards the activated form.

The first available GPCR crystal structure was that of bovine rhodopsin, published in 2000.[45] This structure has a covalently bound ligand (retinal) and differs considerably in sequence from drug relevant GPCRs, but at that time it was still a breakthrough regarding the understanding of receptor structure and mechanism. Recently several more relevant crystal structures of GPCRs have been solved, with medium to high resolution.

† To facilitate a comparison between different GPCRs, the indexing method introduced by Ballesteros and Weinstein is used in this thesis,[44] in which the most conserved residue in every transmembrane (TM) helix is given the index number 50. For example, the Arg residue in the highly conserved DRY motif at the cytoplasmic end of TM3 is denoted $Arg^{3.50}$, the other residues in TM3 are then indexed relative to this position, with the previous residue as $Asp^{3.49}$, and the subsequent as $Tyr^{3.51}$. In addition, the absolute number of each residue in the amino acid sequence is sometimes included.

2.5.2. Monoaminergic receptors and their function

The brain function is regulated by different neurotransmitters, which mainly act via GPCRs. Examples of monoamine neurotransmitters are serotonin, norepinephrine and dopamine (**Figure 5**), which all play central roles in normal brain function.

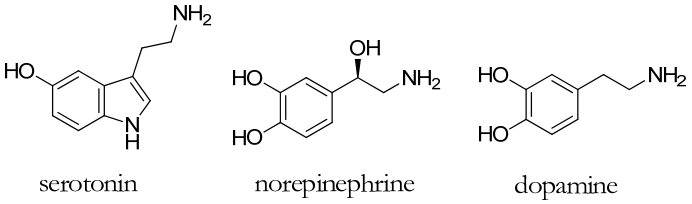

Figure 5. The monoamine neurotransmitters serotonin, norepinephrine and dopamine.

The monoaminergic receptors belong to the class A GPCR superfamily. The receptors show high sequence and structural consistency and may bind the same or similar ligands. Each receptor type is further divided into subfamilies. For example, the serotonin (5-HT) receptors are divided into seven families (5-$HT_{1\text{-}7}$), which can then be further divided into additional subtypes (e.g. 5-$HT_{1A\text{-}F}$). Ligand selectivity between receptor subtypes is a delicate balance, since the receptors are highly conserved in the TM-regions as well in the binding pocket. Several key interactions between the receptors and their agonists have been experimentally verified using mutation studies. An aspartic acid residue in TM3 has been shown to act as a counter ion for the positively charged monoamines.[46-47] Similarly, mutations of a cluster of serine residues in TM5 also greatly reduce monoamine agonist affinities and efficacies.[47-50] Two of these serine residues are more specifically involved in direct binding and appear to form hydrogen bonds with the aromatic hydroxyl groups of norepinephrine, serotonin and dopamine. In addition, a phenylalanine residue in TM6 is essential for high affinity binding of agonists.[51-54]

2.5.3. Dopamine receptors and their function

The physiological functions of 3-OH-tyramine (dopamine), a metabolite of the amino acid tyrosine, were discovered by Carlsson et al.,[55] for more than 50 years ago. Dopamine (DA) acts on receptors which are grouped into two subfamilies, the D_1-like (D_1 and D_5) and the D_2-like (D_2, D_3 and D_4). The division is based on their structure, pharmacology, and signal transduction pathways. The D_1-like receptors couple to the G_s protein and

stimulate adenylate cyclase, which catalyzes the conversion of ATP to cyclic AMP, whereas the D_2-like receptors inhibit this enzyme via the G_i and G_o proteins.[56] The dopamine system is involved in a wide range of fundamental processes such as motor function, reward, cognition and emotion, and is also associated with a variety of neuropsychiatric disorders/diseases such as Parkinson´s disease (PD), schizophrenia and depression. Classical antipsychotic drugs act as DA antagonists and block the DA receptors, while agonists have shown to alleviate the characteristic PD symptoms such as hypokinesia, rigidity and tremor. Dopamine itself (**Figure 5**), administered as its biosynthetic precursor L-DOPA (**Figure 6**), has been used for more than four decades in the treatment of PD. The mixed D_1/D_2 receptor agonist apomorphine,[57] together with the bioavailable D_2 agonists bromocriptine, pergolide, pramipexole, and ropinirole, have all been shown to be useful in the clinic (**Figure 6**).[58] It has been suggested that the ergoline derivatives (e.g. bromocriptine and pergolide) could act as both agonists and antagonists.[59]

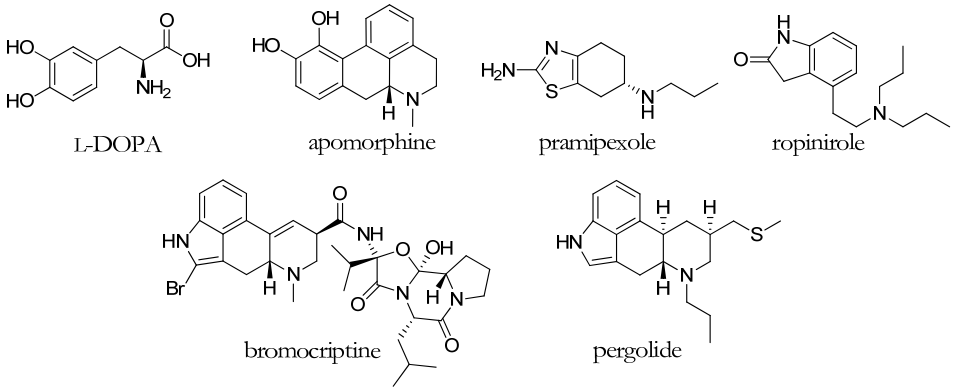

Figure 6. Clinically used antiparkinson agents: the dopamine precursor L-DOPA, together with the D_2 receptor agonists apomorphine, pramipexole, ropinirole, bromocriptine and pergolide.

The role of D_1 receptors (drd1) in treatment of PD was discovered in the 1980s, with the selective agonists SKF38393[60] and CY-208-243[61] (**Figure 7**). These ligands had only modest therapeutic effect, but because both are partial agonists, it led to the hypothesis that the beneficial antiparkinsonian activity depends on their efficacy at drd1. This theory was strengthened by the full and highly selective D_1 receptor agonist ABT-431 (prodrug of A86929, **Figure 7**), which showed the same efficacy as L-DOPA.[62] In addition,

Blanchet et al.[63] reported that the well-known mixed D_1/D_2 full agonist dihydrexidine (DHX, **Figure 7**) also showed a definite motor improvement in patients with PD, but with a narrow therapeutic window. We have used the information from the literature regarding receptors and ligands to increase the understanding of dopamine D_2 and D_1 agonist selectivities.

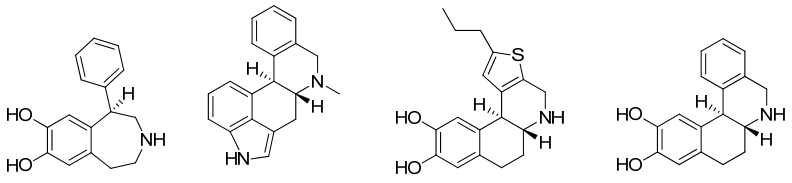

Figure 7. Structures of the D1 receptor agonists SKF38393, CY-208-243, A86929 and DHX which show antiparkinsonian activity.

2.6. Methods in computational drug design

Computational methods are widely used as tools to discover, optimize and study drugs and bioactive compounds. How the ligands interact with their biological targets can be studied in detail using different modeling approaches.

2.6.1. Molecular mechanics calculations

In molecular mechanics (MM) calculations, mathematical functions (the so called force field) are used to describe the potential energy of systems of atoms and molecules and it may be applied on small molecules as well as on macromolecules. The change in energy and the dynamic behavior of a molecule can be described by the fundamental ball-and-spring model (**Figure 8**).[64]

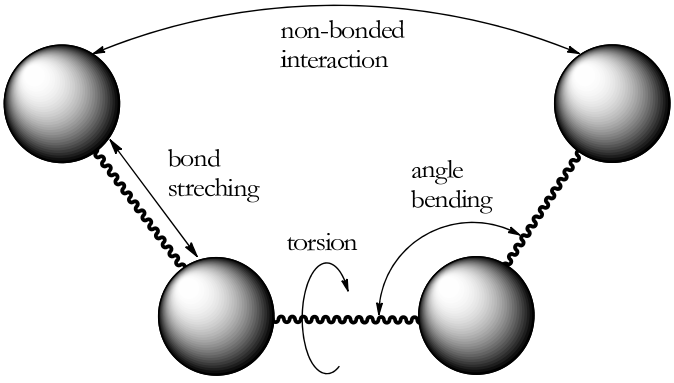

Figure 8. The ball-and-spring model, which is based on the historic physical and chemical analyses of structure and properties. The parameters that contribute to the calculation of the total energy, E_{total}, are denoted as bond stretching, angle bending, torsion and non-bonded interactions.

The mathematical functions and the parameter sets used to describe the potential energy surface (PES), i.e. the energy as a function of the positions of each atom in the system studied, are derived from both experimental work and/or high-level quantum mechanical (QM) calculations. The total energy (E_{total}) of the molecular systems is a sum of energy components which are divided into bond stretching (E_{strech}), angle bending (E_{bend}), non-bonded interactions ($E_{non\text{-}bond}$) including vdW and electrostatic contributions, torsion interaction ($E_{torsion}$) and coupled energy terms ($E_{cross\text{-}term}$) (**Figure 8** and *Eq 4*).

$$E_{total} = \sum_{bonds} E_{strech} + \sum_{angle} E_{bend} + \sum_{non-bond} (E_{vdW} + E_{Elec.}) + \sum_{dihedral} E_{torsion} + \sum E_{cross-term} \quad (Eq\ 4)$$

The ability of the force fields (FFs) to predict molecular properties has gradually been enhanced, as the parameterization has become more accurate during the years. Kollman and co-workers developed AMBER,[65] which is a FF especially applicable for macromolecules. In 1988, Jorgensen et al.[66] developed a FF (OPLS) based on AMBER, that was primarily used for peptides in liquid simulation. Seven years later the same authors released an updated FF where torsion parameters were determined from *ab initio* calculations, to describe approximately 50 small organic molecules and ions.[67] Simultaneously, the MMFF94 FF was developed by Merck Research Laboratories, with the aim to achieve high quality geometries for small drug-like molecules with parameters from high level QM calculations.[68-69] The OPLS FF was further updated and the 2005

version[70] had a greatly expanded coverage of organic and medicinally relevant ligands as the training set of small molecular structures used was considerably larger than those used for the MMFF94[68] and MMFF94s FFs.[69] The OPLS_2005 FF was developed for simulations of protein/ligand-interactions but could also be used for large databases of compounds for which effective potential energy calculations are required.[70]

The molecules can be represented in Cartesian coordinates (x, y, z) or in internal coordinates (Z-matrix), which are interconvertible. The internal coordinates provide a description of each atom in a molecule in terms of its atomic number, bond lengths, bond angles, and dihedral angles using a series of vectors describing atomic orientations in space.

2.6.2. Solvation of molecular systems

The environment surrounding the molecule or molecules may be described in several ways in molecular mechanics calculations. A molecular system can be simulated with no surrounding environment as in a vacuum (gas-phase), but this usually introduces artifacts in the molecular geometry, caused by the electrostatics (charged or polar parts) within the molecules. These polar or charged parts would rather interact with solvent molecules and the presence of such an environment would therefore prevent unlikely molecular conformations. Thus, solvent effects have to be incorporated into a computational treatment of biochemical processes to ensure a reliable description. The use of explicit water molecules is a way to model solvation, however it is computational intensive. As an alternative, methods that use implicit solvation are also available such as the generalized Born solvation model that is highly useful in simulations.[71-72]

2.6.3 Conformational analysis

There are several methods and tools available to explore the PES and identifying low-energy states of a molecular system. Different conformations can be identified by systematic sampling of each torsion angle in a molecule. This method suffers however from the "combinatorial explosion" problem, since the number of conformations increases exponentially with the number of rotatable bonds. Another approach is the low-mode conformational search which explores the low-frequency eigenvectors of the system from any local minima. By using an eigenvector-following technique,[73-74] a saddle

point associated with the minimum could be localized and a second energy minimum with a new eigenvector could be found, etc. Stochastic search methods depend on random assignment of different dihedral angle combinations, followed by an energy minimization step. Several methods are available for random sampling of the conformational space such as simulated annealing[75], Monte Carlo simulation and the random incremental pulse search (RIPS) method.[76]

Monte Carlo (MC) sampling comprises FF based methods that are particularly useful for simulating systems with many coupled degrees of freedom, for example in the case of highly flexible molecules and protein structures. The algorithm is based on random sampling in internal coordinates and compared to molecular dynamics (MD) calculations the MC-methods sample the conformational space more efficiently. In combination with Metropolis sampling,[77] MC generates Boltzmann weighted conformational ensembles that can be used for calculating thermodynamic observables for the system.

There are methods available aimed to speed up conformational searches for large databases of molecules. Conformational import does not sample the whole molecule conformations but identifies and assembles fragment conformations from a database of pregenerated fragment conformations.

2.6.4. Structure based design

Design of ligands that relies on knowledge of the 3D structure of the macromolecular target is known as structure-based design. Macromolecular structures are experimentally determined by nuclear magnetic resonance (NMR) spectroscopy or X-ray crystallography. The latter method gives in general better structural resolution than the determinations by NMR spectroscopy or modeled with guidance from structures of related proteins, as described in the following section.

2.6.4.1. Homology modeling

Homology modeling, also known as comparative modeling, is a method used when the target protein structure is not known, but the structure of a related protein is available. The method relies on the evolutionary fact that homologous proteins with similar amino acid sequences, most likely have similar 3D-structures.[78] The homologous proteins often

contain regions that retain the same general 3D-structure and regions that differ. The geometrical quality of the constructed model depends partly on the similarity of the sequences, the resolution of the template structure and in some cases on the conformational state of the template structure. There are several softwares available to construct homology models such as Modeller,[79] Prime,[80] SWISS-MODEL,[81] etc., however in this thesis we have used ICM[82] and MOE,[83] the description below focuses on the latter method.

There are usually four steps in the homology modeling procedure:

- *Template selection* – Several methods are available to identify suitable protein templates, which are sufficiently close in evolution to result in a reliable homology model. The template may belong to a homologous protein family or have a function similar to that of the query sequence. It is also possible to pick different template structures to different regions when more than one template structure is available.
- *Sequence alignment* – This step is often performed together with the template selection, as the most common methods of identifying templates rely on the production of sequence alignments. For greater credibility of the alignment, several related sequences can be compared in a multiple sequence alignment. The alignments must still, in many cases, be manually checked and adjusted to be consistent with structural and experimental data, if such are available. An error in alignment will severely impair the quality the model in that region.
- *Model generation/model refinement* – In the most applied method, and in that used in this thesis, all atom geometries of the conserved residues are copied from the template into the model while only the backbone geometries are copied in the non-conserved parts. In those regions where the model has no template structure (gaps), typically found in loops, the program searches for fragments in PDB[2] to anchor up to the already modeled parts. Once all the loop fragments have been chosen, the side chains are modeled. Side chain data are assembled from an extensive rotamer library generated by systematic clustering of PDB data. A deterministic procedure based on Unary Quadratic Optimization (UQO)[84] is

then run to select an optimal side chain packing. When all backbone segments and side chain conformations are modeled, hydrogen atoms are added to complete the valence requirements. The models are then submitted to a series of energy minimizations before the final preparation of the models are scored and written to an output database.

- *Evaluation of the protein model* – Protein geometry evaluation tools can be used in order to confirm that the geometric quality of the selected models is reasonably consistent with typical values found in crystal structures. There are geometry evaluation tools implemented in the MOE software,[83] but there are also several other evaluation programs available, e.g. Procheck.[85] Manual adjustments to the structure due to for example errors in the sequence alignment may be necessary, particularly in the loop areas, followed by a rebuilding of the model.

2.6.5. Ligand based design

Ligand based design methods are typically used when the three-dimensional (3D) structure of the target protein is unknown, or as a complement to structure based methods. The ligand based methods require the use of several compounds with the desired biological profile, these compounds are used to gain information regarding the 3D rearrangement of functional groups in the ligands in order to e.g. guide the design of novel ligands.

2.6.5.1. Pharmacophore modeling

Pharmacophore modeling is a useful method to extract important structural properties from a set of ligands with a shared biological profile. The pharmacophore can be considered as the largest common denominator shared by a set of active ligands. Properties of the ligands important for target protein interactions can be referred to as pharmacophore features and correspond to a spatial arrangement of interacting functional groups (within or outside the ligands). The pharmacophore features will reflect important interactions with amino acids in the binding site and thereby image the protein binding pocket. Ligands which bind to a protein may have various inherent degrees of freedom, but the conformational energies of strong binders are generally within 3 kcal·mol^{-1} from the global minimum conformation.[86] In addition, it has been suggested that each 1.4

kcal·mol^{-1} of increased energy decreases the binding affinity 10-fold.[86] Therefore an ensemble of low-energy conformations for each ligand is needed to be able to identify the bioactive ligand conformations. In the pharmacophore modeling process it is strategically best to start from the most rigid structures and then try to superimpose the more flexible compounds into the pharmacophore model. The active ligands should not only be conformationally rigid but also structurally diverse. In addition, inactive compounds resembling the actives should be included in the procedure to increase the chances to obtain a true bioactive 3D pharmacophore. When as many as possible of the active ligands fit into the pharmacophore model one may try to exclude inactive ligands, if such are available, with the aim to make the model selective. The inactives can be excluded by not hitting essential pharmacophore features or entering into forbidden areas/volumes, which no parts of the ligands are allowed to occupy.

Once a sufficiently selective model has been derived it can be used to search for existing compounds that contain the same pharmacophore elements and thereby may show similar activity. Furthermore, the pharmacophore model may help to interpret the existing structure activity data and generate ideas to design new potentially active candidates.

The software packages available for pharmacophore modeling differ mainly in how the ligands are superimposed. The first commercial software for pharmacophore discovery was Catalyst,[87] which uses a simplified version of the CHARMm[88] force field to evaluate the conformational space of ligands. The conformational search in Catalyst uses a "poling" algorithm to maximally span the accessible conformational space of a molecule and not necessarily only the local minima.[89] The recommended energy threshold is rather high (20 kcal·mol^{-1}), and the high energy cut-off allows odd conformations to also match the pharmacophore. Other pharmacophore generating tools are also available, such as Phase[90] and LigandScout.[91]

In the pharmacophore modeling tool in the MOE program,[83] a pharmacophore annotation scheme is used to assign pharmacophore points (such as H-bond donor and/or acceptor, hydrophobic atom, etc.) from a 3D conformation of a ligand. These points can be divided into three broad categories:

- *Atom annotations* - located on an atom in the ligand, such as "H-bond donor or acceptor" or "cation" and typically indicate a functional group in a ligand involved in protein-ligand binding.
- *Centroid annotations* - located at the geometric center of a subset of the atoms in a ligand. For example, an aromatic ring annotation will be located at the centroid of the ring.
- *Projected annotations* - for example positioned along hydrogen bond directions and are used to annotate the position of possible hydrogen bond interaction points.

The pharmacophoric features have a spherical shape and the size of the spheres can be fine-tuned manually to achieve a model that fits the experimental data. The pharmacophore hits are ranked with respect to the RMSD calculated from the centers of the pharmacophore features to the corresponding annotation point from the hitting ligand conformation. The program includes an RMSD cut-off which can be set by the user, but the relative conformational energy of the ligand is a more informative value if the hit is sufficiently good or not. It is also possible to add volume constrains, such as *excluded volumes* where no matching heavy atoms are permitted, *exterior volumes* where no predefined heavy atoms are permitted outside the volume and *included volumes* where at least one specified atom type must be positioned inside the volume. In addition, logical constraints for feature matches such as “and” and “or”, together with priority settings such as *partial-* or *essential match*, can be used to further refine the pharmacophore model. The generated model may be validated by verifying/falsifying hits experimentally.

3. Dopamine D_2 agonist pharmacophore and receptor modeling

During the years, dopamine D_2 receptor (drd2) function and agonist binding have been extensively studied using various techniques. Important amino acids for agonist binding have been pointed out using site-directed mutagenesis combined with binding studies. As in all drug relevant monoaminergic receptors the dopamine D_2 receptor has an aspartic acid in TM3 (Asp103$^{3.32}$)[46-47] which interacts with the amino function of agonists. There is a cluster of serine residues (Ser193$^{5.42}$, Ser194$^{5.43}$ and Ser197$^{5.46}$)[48-50] interacting with hydrogen bonding substituents in the aromatic ring of the agonists. A hydrophobic face in TM6 (Trp386$^{6.48}$, Phe389$^{6.51}$, Phe390$^{6.52}$ and His393$^{6.55}$),[51, 92] has also been identified to be important for dopamine agonist interactions. Shi and Javitch[93] found that two amino acids (Ile184 and Asn186) in the second extracellular loop (EC2) that lines the binding crevice are pointing downwards into the binding pocket and are important for ligand binding. As all monoaminergic GPCRs, drd2 has a disulfide bridge (EC2-SS-TM3) that connects a cysteine residue in EC2 (Cys182 in drd2) with a cysteine in TM3 (Cys107$^{3.25}$). It has been shown that disruption of this disulfide bond in GPCRs dramatically decreases ligand binding,[94] or could destabilize the high-affinity state of the receptor.[95]

3.1 Dopamine D_2 agonist pharmacophore models

Early dopamine D_2 receptor agonist pharmacophore models were based on the following features: i) the amino function (including the direction of the hydrogen bond), ii) the hydrogen bond acceptor/donor site, and iii) the aromatic site. These features were used for the superimposition of a set of different agonists in order to identify an agonist based pharmacophore.[96-101] These first reported approaches focused mostly on the amino function and the hydrogen bonding features of the agonists, and they only included a limited training set of ligands. Later Cho et al.[51] demonstrated that a specific phenylalanine residue in drd2 (Phe390$^{6.52}$) was important not only for binding affinity, but also for receptor activation. This was also shown to be the case in several other GPCRs, e.g. Parrish et al. suggested a π–π-interaction between the agonist and the corresponding

phenylalanine in the 5-HT_{2A} receptor.[102] Therefore alignment of the aromatic ring of the different agonists in the pharmacophore ligand training set is of special importance.

There are many D_2 agonists known from different structural classes, such as phenethylamines, apomorphines, aminotetralines and benzoquinolines, with various affinities and efficacies. The predictivity of a pharmacophore model is highly dependent on the ligands included in the construction of the model. We have therefore selected relatively rigid agonist from the different classes which demonstrated high efficacy and high binding affinity (actives), together with structurally similar inactives. The inactives could be non-binders, inverse agonists, antagonists or low intrinsic partial agonists.

Many of the inactives are enantiomers to the actives or are substituted differently compared to the actives. The actives do not necessarily have to be selective for the D_2 receptor, as long as they fulfill the criteria regarding their pharmacological profile and conformational rigidity. In addition, some structurally related potent partial agonists have also been included to generate a deeper understanding of structure-efficacy relationships. The compounds included in the set are shown in **Figure 9**.

3.1.1 The construction of a new ligand based dopamine D_2 agonist pharmacophore model (Paper I)

In this project, the initial D_2 agonist pharmacophore model was constructed from low-energy conformers of two superimposed full D_2 agonists (*R*-NPA[57] (**1**) (ΔE = 0.015 kcal·mol^{-1}) and talipexole[103-104] (**2**) (ΔE = 0.007 kcal·mol^{-1}) (**Figure 10a**). The superimposition was made using a SEAL[105] alignment and the initial pharmacophore model consisted of i) a projected feature representing the aspartic acid residue in TM3 (Asp-TM3), ii) two projected features representing the serine residues in TM5 (Ser-TM5 A and B), iii) a combined feature arrangement defining the aromatic system (Aro) and, iv) a hydrophobic inclusion volume (**Figure 10a**). The Asp-TM3 feature was defined as a projected hydrogen bond donor feature, since the amino function interacts with the carboxylate via a charged assisted hydrogen bond. The Ser-TM5 features act both as hydrogen bond acceptors and donors. The Aro system consists of an aromatic centroid feature together with two ring normals which determine the orientation of the aromatic plane.

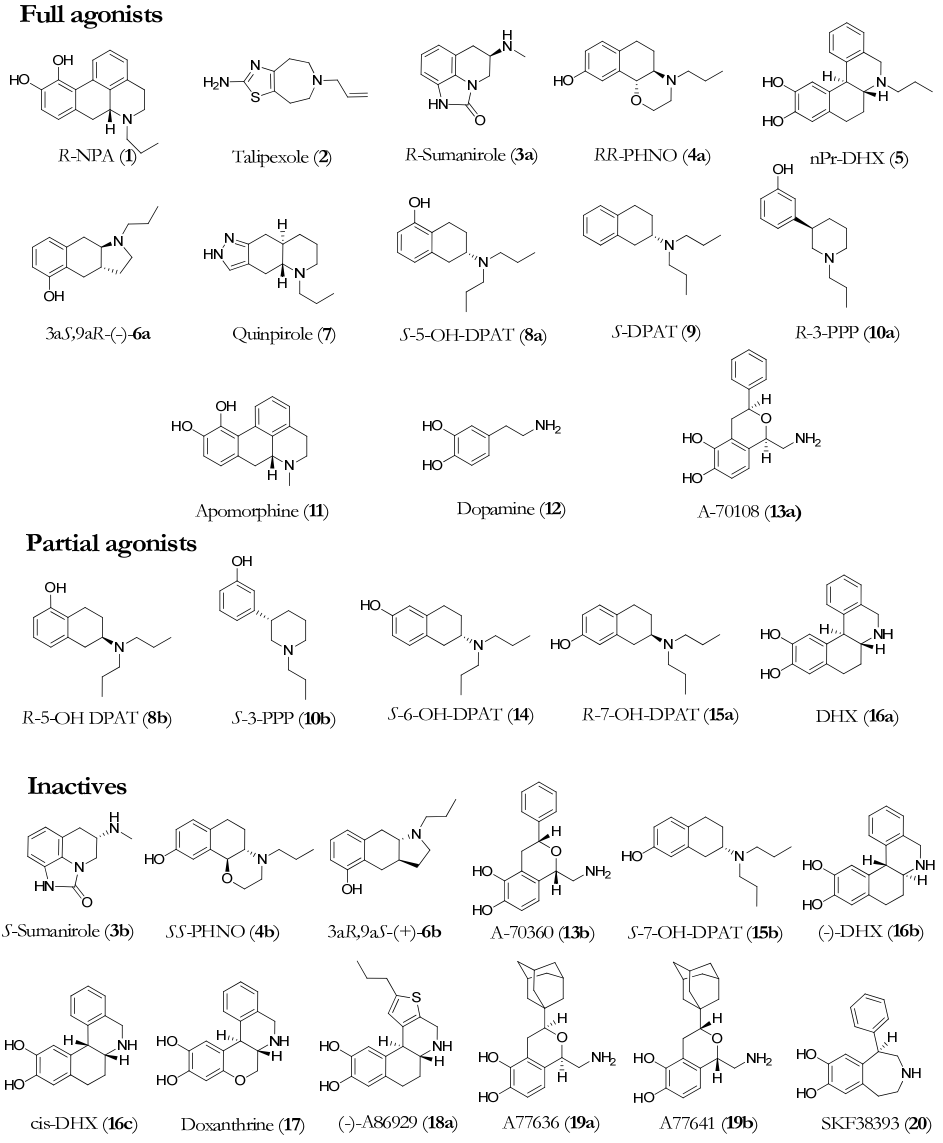

Figure 9. Selected D_2 receptor full agonists (**1–13a**), partial agonists (**8b, 10b, 14, 15a** and **16a**) and structurally related inactives (**3b**, **4b**, **6b**, **13b**, and **15b-20**).

The two hydrogen bond 'acceptor *and* donor' features (A and B Ser-TM5, **Figure 10**a) in the initial model were replaced with one 'acceptor *or* donor' feature, which allows for interactions with non-hydroxy containing functional groups such as carbonyl oxygens and donating N-H groups (**Figure 9**). The position of the new Ser-TM5 feature was fine-

tuned (**Figure 10b**). In addition, its priority was changed to be essential, from being either one of the Ser-TM5 features. In this refined model the D_2 agonist characteristic hydrophobic inclusion volume (Hyd) was removed (**Figure 10b**), to prevent it from being a too strong determinant for the D_2/D_1 agonist selectivity. It was not necessary for discrimination and by its removal we wished to obtain insights in other causes for agonist selectivity than the propyl pocket. The removal of the Hyd-volume resulted in pharmacophore hits where the protonated amino function interacted with the Ser-TM5 feature, but by the inclusion of a cation feature the amino function could be correctly oriented. The cation feature was located near Asp-TM3 and the radius of the feature was large to allow Asp-TM3 hits from different directions.

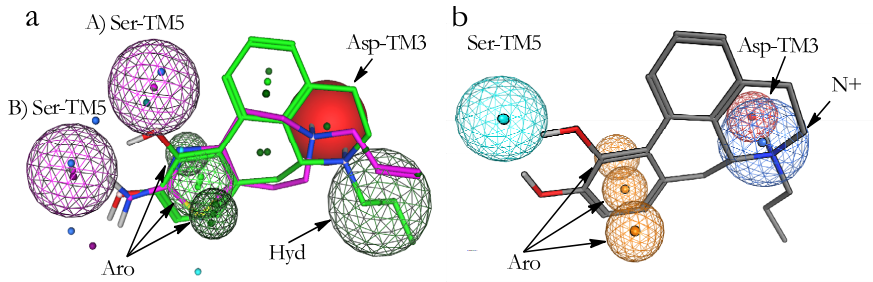

Figure 10. a) The initial dopamine D_2 agonist model based on the superimposition of the full agonists *R*-NPA (**1**; green) and talipexole (**2**; purple). The pharmacophore consists of two projected hydrogen bond acceptor and donor features (Ser-TM5), a hydrogen bond donor feature that interacts with the protonated amino function (Asp-TM3), a hydrophobic feature (Hyd), and a combined feature that defines the aromatic system (Aro). b) The refined D_2 agonist pharmacophore model together with the selective D_2 agonist *R*-NPA (**1**). The model includes Asp-TM3, which describes the projected anion. The annotation points are: Ser-TM5, N+, Asp-TM3 and Aro (the aromatic system).

The pharmacophore model was screened against four differently generated ensembles of conformations of the D_2 ligands (Table A1 in Appendix and MMFF94(S) and OPLS_2005 results in **Table 1**). All active ligands except *S*-DPAT (**9**) (12/13) fitted the pharmacophore model, **9** did not fit as it is not capable to interact with the essential Ser-TM-5 feature. Furthermore two out of four partial agonists (2/4, *S*-6- (**14**) and *R*-7-OH-DPAT (**15a**)) and eight out of twelve inactives did hit the pharmacophore. The four inactives that missed were *S*,*S*-PHNO (**4b**), 3a*R*,9a*S*-(+)-**6b**, *S*-7-OH-DPAT (**15b**) and *cis*-DHX (1**6c**). To retrieve selectivity, i.e. to exclude the inactives, we introduced exclusion

volumes. The volumes were added one by one and their positions and sizes were fine-tuned to exclude all conformations of the inactives, but still include conformations of active compounds.

The chromane-like DHX analog doxanthrine (**17**; **Figure 9**) shows considerably lower affinity for the D_2 receptor than DHX (**16a**), which might indicate that the presence of a more hydrophilic ether function results in loss of activity. Therefore, a volume excluding oxygen (Excl O) in this position was added to discriminate **17** (**Figure 11**). The final ligand based D_2 agonist pharmacophore model succeeded to include all but **9** of the full agonists (12/13 hits), two out of four partial agonists (2/4 hits) while all inactives (0/12 hits) were excluded (**Table 1**).

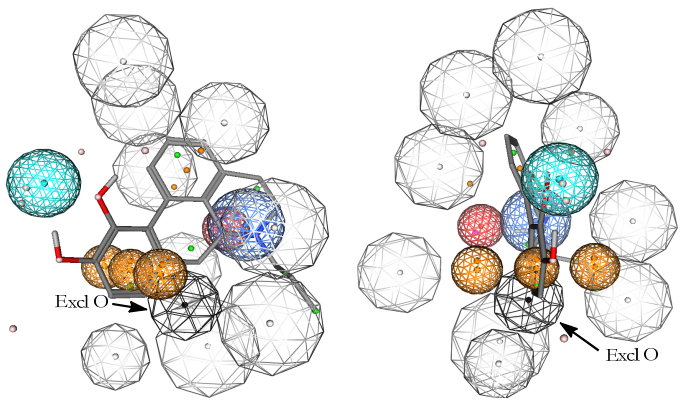

Figure 11. Two orthogonal views of the final ligand based D_2 agonist pharmacophore model, together with the D_2 selective agonist *R*-NPA (**1**). The grey spheres represent the excluding volumes and the black the excluding oxygen volume. The feature color coding is the same as in **Figure 10**.

3.1.2. The refinement of the dopamine D_2 agonist pharmacophore model guided by the receptor model (Paper II)

The selective D_2 agonist pharmacophore model was superimposed into a structure model of the D_2 receptor to compare the positioning of amino acids in the binding pocket with the pharmacophoric features and excluded volumes (the receptor modeling details are described below in section 3.2.2.). The geometry of the feature arrangement in the pharmacophore was in good agreement with the structure model, with the exception of the Ser-TM5 feature, which did not coincide with the serine residues but was instead located more towards the extracellular side close to Val190$^{5.39}$ (**Figure 12**). The

positioning of excluded volumes differed also compared to the shape of the binding site. This is probably due to the fact that the initial pharmacophore approach is strictly guided by the ligands. We therefore decided to move the Ser-TM5 feature to be more consistent with the Ser193$^{5.42}$ position in the 3D receptor model and reposition the excluded volumes to better match the shape of the binding pocket. The new Ser-TM5 feature was positioned deeper in the binding crevice based on projected hydrogen bond annotation points generated from the pharmacophore hits of low-energy conformers of full D_2 receptor agonists.

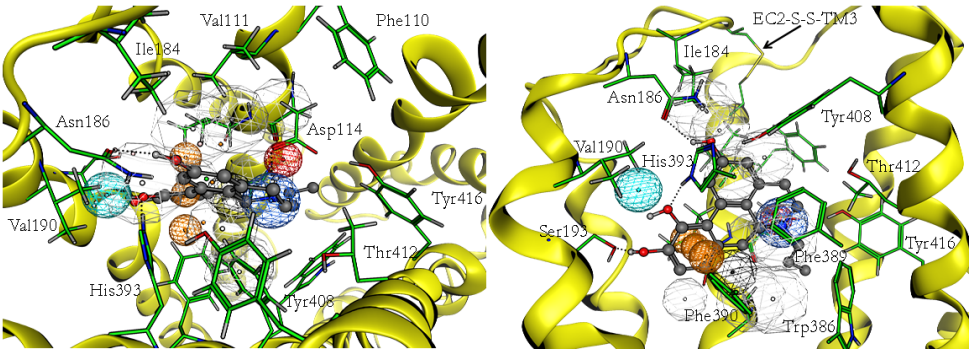

Figure 12. Two orthogonal views of the ligand based selective dopamine D_2 agonist pharmacophore model superimposed into the D_2 homology model, with the selective agonist 2-OH-*R*-NPA present. The backbone ribbon of the transmembrane helix 6 (TM6) is not shown on the side view (right), but the side chains of the interacting amino acids Phe389$^{6.51}$, Phe390$^{6.52}$, andTrp386$^{6.48}$ are still included. The positioning of the anion feature (red) superimposes well with the aspartic acid Asp114$^{3.32}$, as well as the position and direction of the aromatic system (orange), while the hydrogen bonding feature, Ser-TM5, together with the excluded volumes, do not match the receptor model.

The size and position of the features were fine-tuned until all full agonists in the set fitted into the model. The priority of the hydrogen bond donor/acceptor feature was also redefined from being essential to optional, since hydrogen bonding does not seem to be crucial for obtaining a maximal D_2 receptor intrinsic activity. The other features were kept as essential, which means that they must be matched. Excluded volumes were added to cover the hydrogen atoms in the amino acid residues surrounding the ligand to reflect the shape of the binding pocket. The selected hydrogens were bound to amino acids within 3 Å from the ligand position (the D_2 selective agonist, *R*-2-OH-NPA), including those involved in hydrogen bonding. The initial radii of the excluded volumes were selected

based on the van der Waals radii (vdWr) proposed by Bondi,[106] (i.e., 1.2 Å for aliphatic and 1.0 Å for aromatic hydrogen atoms). The vdWr for hydrogen atoms in hydroxy and amino groups are not defined by Bondi, but were set at the same radii as the aromatic hydrogens. The sizes of the excluded volumes were gradually increased until the model was sufficiently selective between actives and inactives. The final diameters were 2.0 Å for aliphatic and 1.8 Å for the aromatic. Furthermore, excluded volumes with a diameter of 2.5 Å were introduced at the centers of mass of the aromatic rings, to avoid perpendicular clashes between the ligands and the receptor. The alignment of the feature part of the pharmacophore model in relation to the set of new excluded volumes derived from the receptor model was further tuned manually and evaluated by the hit rate of the ligand training set. The oxygen excluding volume (Excl O) was reintroduced to discriminate **17**.

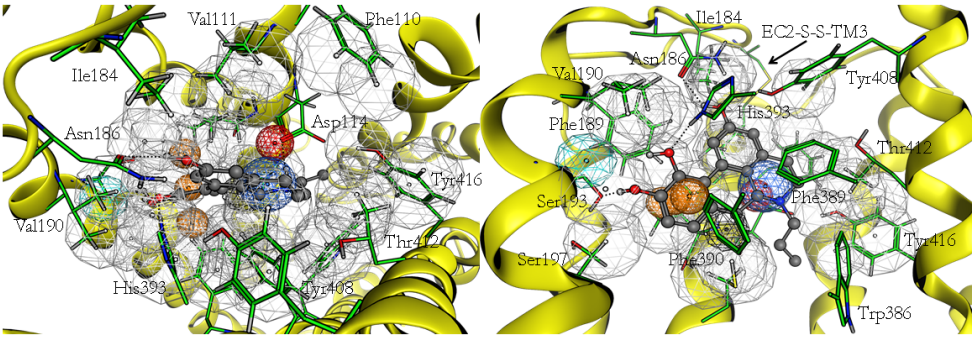

Figure 13. Top view (left) and side view (right) of the new pharmacophore model based on the agonist-induced dopamine D_2 homology model, with *R*-2-OH-NPA present in the binding site. The backbone ribbon of TM6 and the corresponding excluded volumes are not shown. The conformation of *R*-2-OH-NPA is taken from the ligand-receptor homology model complex, whereas the relative positions of the pharmacophore features are tuned to generate the best hit rate.

The structure based agonist pharmacophore model (**Figure 13**) was screened against the set of D_2 ligands (13 full agonists, 5 partial agonists and 12 inactives, **Figure 9**) and when using the OPLS_2005 generated ensemble of conformations all except two full agonists (*R*-3-PPP (**10a**) and A70108 (**13a**), 11/13), all but one of the partial agonists (*S*-3-PPP (**10b**), 4/5) and only one of the inactive (*S*-7-OH-DPAT (**15b**), 1/12), did fit into the pharmacophore model (**Table 1**). The screen of MMFF(S) generated conformations showed similar hit rate (11/13, 3/5 and 1/12, **Table 1**). The main reason that neither enantiomer of 3-PPP did fit the model is the perpendicular orientation between the

piperidine and phenol rings in low-energy conformations of 3-PPP. Liljefors and Wikström have shown that the 3-PPP enantiomers require a conformational change for binding.[107] A70108 (**13a**, **Figure 9**), which also has a single bonded phenyl ring attached to an isochromane scaffold, shows a similar orientation of the ring systems as the 3-PPP enantiomers. This might explain the relatively low D_2 receptor affinity for these three compounds.

Since the pharmacophore model was superimposed into the generated drd2 structure model the pharmacophore ligand hits could be interpreted with respect to their ability to interact with the specific D_2 agonist key interactions. Cox et al.[50] and Wiens et al.[48] have done Ser→Ala mutation studies on the serine residues in TM5 and concluded that Ser193$^{5.42}$ is most important for binding of catechol-containing full D_2 agonists. The efficacy for inhibition of adenylate cyclase stimulation of *R*-NPA (**1**), the non-catechol containing agonist quinpirole (**7**) and the partial agonist *R*-7-OH-DPAT (**15a**) was not affected by any of these Ser→Ala mutated receptors. Interestingly, Tschammer et al.[92] showed that the binding of **7** and DA (**12**) are negatively affected by a His393$^{6.55}$→Ala mutation, but not by a His393$^{6.55}$→Phe mutation. We therefore decided to evaluate the best hit of each compound in the pharmacophore model by measuring the hydrogen bond distances and angles between the ligand and the amino acids Ser193$^{5.42}$ and His393$^{6.55}$. The optimal distance for hydrogen bonding is ~2.8 Å between the heavy atoms, but since the receptor is flexible we consider distances between 2.4 and 3.8 Å to be acceptable. The angle between the heavy atom and the hydrogen of the ligand to the oxygen in the interacting amino acid (N/O···H···O(Ser193$^{5.42}$) and N/O···H-N(His393$^{6.55}$) should ideally be 180±40º, but could as mentioned before be down to 120º if the distances are appropriate. These measurements were done for the OPLS generated conformations and the results are shown in **Table 1**. Worth to notice is that the pharmacophore hit of the inactive ligand *S*-7-OH-DPAT (**15b**) was unable to make proper hydrogen bonding interactions with Ser193$^{5.42}$ or no interactions at all with His393$^{6.55}$. Several of the full agonists such as R-NPA (**1**) were oriented in a position able to form hydrogen bonds with both Ser193$^{5.42}$ and His393$^{6.55}$. The partial agonist DHX (**16a**) interacted with His393$^{6.55}$ at a suboptimal distance (4.5 Å and 146º), but it can form hydrogen bonds to Ser193$^{5.42}$ with both catechol hydroxy groups (**Table 1**).

Table 1. Results of the ligand and structure guided D_2 agonist pharmacophore model search of two different ensembles of generated conformations.

Ligand		Structure guided pharmacophore model								Ligand based pharmacophore model					
		MOE stochastic search Born solvation, MMFF94(S)[a]			*MacroModel serial torsion search GB/SA solvation, OPLS2005*[b]					*MOE stochastic search Born solvation, MMFF94(S)*[a]			*MacroModel serial torsion search GB/SA solvation, OPLS2005*[b]		
		ΔE[c]	RMSD[d]	#c/#h[e]	ΔE[c]	RMSD[d]	Ser193 d[Å](ang[°])[f,h]	His393 d[Å](ang[°])[g,h]	#c/#h[e]	ΔE[c]	RMSD[d]	#c/#h[e]	ΔE[c]	RMSD[h]	#c/#h[e]
(R)-NPA (**1**)[i]	Full	0.0	0.26	12/3	0.6	0.22	**m3.7(129)** p2.4(163)	3.6(157)	21/11	0.0	0.59	12/6	0.0	0.45	21/19
Talipexole (**2**)[i]	Full	0.0	0.43	44/28	0.0	0.43	2.4(171)	**4.1(151)**	28/15	0.0	0.54	44/22	0.0	0.51	28/14
R-Sumanirole (**3a**)	Full	0.0	0.26	5/1	0.3	0.32			3/1	0.0	0.32	5/2	0.0	0.23	3/2
RR-PHNO (**4a**)	Full	0.0	0.3	6/1	1.3	0.30	2.7(144)	**4.6(152)**	12/6	0.0	0.51	6/4	0.0	0.44	57/24
nPr-DHX (**5**)[i]	Full	0.4	0.39	3/1	0.0	0.36	m3.0(147) **p2.9(139)**	**4.5(144)**	57/6	0.4	0.47	3/1	0.0	0.50	12/12
3a*S*,9a*R*-(-)-**6a**[i]	Full	0.0	0.25	5/3	0.0	0.25	**3.7(128)**	3.6(158)	12/6	0.0	0.53	5/5	0.0	0.54	12/12
Quinpirole (**7**)[i]	Full	0.1	0.26	5/1	1,1	0.21		**150(4.4)**	9/4	0.0	0.38	5/5	0.0	0.36	9/7
S-5-OH-DPAT (**8a**)	Full	1.7	0.26	78/12	2.2	0.26	**3.7(128)**	3.6(164)	140/11	1.7	0.57	78/21	2.1	0.57	140/30
S-DPAT (**9**)	Full	1.7	0.27	79/12	2.2	0.27			79/6						
R-3-PPP (**10a**)[i]	Full			26/0					43/0	3.5	0.68	26/3			43/0
Apomorphine (**11**)	Full	0.0	0.19	2/1	0.0	0.21	2.4(164)	3.6(157)	4/4	0.0	0.56	2/1	0.0	0.47	4/4
Dopamine (**12**)	Full	0.0	0.57	8/4	0.0	0.58	m3.8(137) p2.6(145)	m3.8(167)	20/12	0.0	0.66	8/3	0.0	0.61	20/6
A70108 (**13a**)	Full			6/0					10/0	2.2	0.57	6/2	2.8	0.58	10/1
R-5-OH-DPAT (**8b**)	Partial	0.0	0.67	75/13	2.3	0.66	**3.5(132)**	3.7(158)	140/14			75/0			140/0
S-3-PPP[d] (**10b**)	Partial			18/0					54/0			18/0			54/0
S-6-OH-DPAT (**14**)	Partial	1.7	0.26	82/14	2.2	0.27	**4.0(179)**		154/14	1.7	0.53	82/22	2.1	0.54	154/34
R-7-OH-DPAT (**15a**)	Partial	0.0	0.67	84/13	2.2	0.27	2.6(148)		152/16	1.8	0.65	84/16	2.1	0.63	152/28
DHX (**16a**)	Partial				0.0	0.32	m2.9(150) p2.8(143)								
S-Sumanirole (**3b**)	Inactive			5/0					3/0			5/0	1.5	0.62	3/1
SS-PHNO (**4b**)[i]	Inactive			6/0					16/0			6/0			16/0
3a*R*,9a*S*-(+)-**6b**[i]	Inactive			5/0					12/0			5/0			12/0
A70360 (**13b**)	Inactive			5/0					15/0			5/0			15/0
S-7-OH-DPAT (**15b**)	Inactive	1.7	0.67	79/12	2.8	0.25	**3.8(128)**		151/5			79/0			151/0
(-)-DHX (**16b**)	Inactive			2/0					14/0			2/0			14/0
cis-DHX (**16c**)	Inactive			6/0					12/0			6/0			12/0
Doxanthrine (**17**)	Inactive			2/0					16/0			2/0			16/0
(+)-A86929 (**18a**)	Inactive			11/0					48/0			11/0	0.0	0.64	48/23
A77636 (**19a**)	Inactive			3/0					11/0			3/0			11/0
A77641 (**19b**)	Inactive			3/0					11/0			3/0			11/0
SKF-38393 (**20**)	Inactive			5/0					22/0			5/0			22/0

[a]The energy cutoff for conformations generated in MOE is 4 kcal mol^{-1}. [b]The energy cutoff for conformations generated in MacroModel is 16.7 kJ mol^{-1} (~4 kcal mol^{-1}). [c]The relative energy [kcal mol^{-1}] of the conformer that fit the pharmacophore model, related to the most stable conformer in the ensemble. [d]Root of the mean square distance between the center of the pharmacophore features and their matching ligand annotation points. [e]#c: number of conformations generated using the assigned method; #h: number of conformations that hit the pharmacophore model. [f]Hydrogen bond distance and angle between heavy atoms of Ser193 of the receptor and the best hits in the new pharmacophore model (O···H···O). [g]Hydrogen bond distance and angle between heavy atoms of His393 of the receptor and the hydrogen bond acceptor (A) in the best hits in the structure based pharmacophore model (A···H-N). [h]The *para* and *meta* positions of the hydroxy groups in the dopamine substructure are indicated by p and m, respectively; values in boldface are just outside the permitted values (2.4–3.8 Å and 180±40°). [i]The tertiary amine is considered chiral, and two different configurations have been used in the modeling.

DHX lacked efficacy for inhibition of adenylate cyclase via the Ser193$^{5.42}$→Ala mutated receptor, while the intrinsic activities were unaffected for 1 and the non-catecholamine agonists **7** and *R*-7-OH-DPAT (**15a**).[48] The serine mutation may change the binding mode for DHX due to hydrogen bond formation between the meta-hydroxy group and His393$^{6.55}$ and thereby a loss of the important face-to-edge π-π interaction with Phe390$^{6.52}$. As the hit priority of the Ser-TM5 feature was changed to optional, also the full agonist *S*-DPAT (**9**) could fit into the model.

3.2. Agonist-bound dopamine D_2 receptor structure modeling

As the D_2 receptor has not been crystallized a structure model had to be constructed. To circumvent the lack of relevant template structures, methods based on *ab initio* prediction of all types of membrane protein structures (Rosetta[108]) including GPCRs (PREDICT[109] and MembStruk[110]) have been developed. Shacham et al.[109] applied their PREDICT method on drd2 and performed a screening study showing an enhanced enrichment of a set of 43 D_2 ligands seeded into 10,000 drug-like ligands, relative a random screening. MembStruk was used to generate models of drd2 to study both antagonist and agonist binding, but only a limited set of structures was included, especially agonists.[111] Furthermore, not all experimental data available regarding mutations and agonist binding were considered. In order to get more relevant protein binding site geometries Evers and Klebe invented a homology modeling procedure, based on a bound ligand forming restraints in the binding site.[112] We applied a similar strategy by including an agonist in the binding crevice during the modeling to generate a drd2 structure model that represents the agonist bound state.

There are several available GPCR structures that could be used as a template for prediction of drd2, e.g. the dopamine D_3 receptor (drd3),[113] the adenosine A_{2A}[114] receptor or the adrenergic β_1-,[29] or β_2-[28, 30, 115] receptor structures. It could be expected that drd3 should be a natural choice because it has the highest sequence homology with drd2, but as the ligand used in the structure determination (eticlopride) binds rather shallow in the binding crevice and does not interact with the typical agonist interacting amino acids it may not be the most suitable template. In addition, the ligand used for the drd3 crystallization is an antagonist and as we were interested in the receptor/agonist

interactions, that might also be a drawback. The large sequence similarity between drd3 and drd2 (78%) can therefore be a disadvantage as many of the homology modeling tools use an algorithm where the homology model inherits the exact geometry of conserved amino acids.

Eleven X-ray structures of GPCRs with an agonist bound or claimed to be in an active state have been published recently; two ligand-free opsin structures,[116-117] two β_2,[28, 30] five β_1[29] adrenergic, and two adenosine A_{2A}[118] structures. The active versus the inactive β_2 receptor structures differ relatively little in the binding pocket, instead they differ considerably towards the cytosolic side. The resolution of the two active adrb2 structures (3.5 Å, PDB-code 3PDS[28] and 3P0G[30]) is lower compared to the previously solved β_2 structure crystallized with an inverse agonist present (2.4 Å, 2RH1[115]). The best β_1 structure has a high resolution (2.6 Å), but according to Warne et al.[29] the receptor adopts an inactive conformation despite the bound agonist. The agonist bound adenosine A_{2A} structure 2YDV[118] has also a high resolution, 2.6 Å, but its homology with drd2 is rather low (31% in the TM region except IC3). At the time for this investigation the 2RH1 structure was considered the most suitable template for homology modeling (section *3.2.2.*).

3.2.1. A semi-empirical helix docking method with ligand present (Paper IV)

A semi-empirical 7TM modeling method was developed which is based on repacking of the helices of a homology model using Monte Carlo sampling in torsion space, followed by ranking based on their structural, geometrical and ligand-binding properties. The main purpose of this method was to model GPCRs with focus on the binding pocket and to analyze agonist binding, mainly to the dopamine D_2 receptor. The method is Monte Carlo based and the molecular system is defined in torsion space and the positioning and orientation of each helix is controlled by only six variables (**Figure 14**).[119]

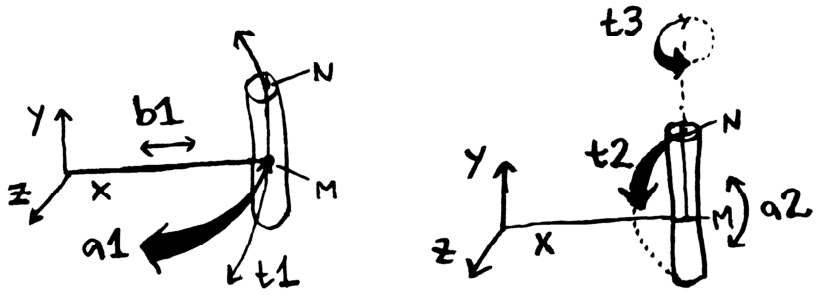

Figure 14. The position and orientation of each helix is determined by six variables only in the torsion space representation, which makes geometry optimizations more efficient.[119] Labels indicate the *N*-terminus (N), the center of mass of the helix (M), the coordinate system axes (x, y, *z*) and virtual variables (a1, b1, t1, a2, t2, t3).

In the modeling procedure the loops were cut out to make the conformational sampling more efficient, but these could be added back when a desired model was generated. The bundle consisting of seven helices is expanded and randomly displaced, i.e. each helix was moved by a random distance (0-5 Å) away from the bundle center in the membrane plane, tilted with respect to its center (0±20 degrees) and rotated around the helical axis (0±30 degrees). To bring the helix bundle back weak initial restraints were introduced to the original homology model and to a ligand present. The ligand guided the receptor towards a chosen conformational state, i.e. for example agonist (active) or inverse agonist-induced (inactive) states.

In order to validate the method we constructed a β_1 adrenergic receptor model in complex with *S*-cyanopindolol, which could then be compared with the crystal structure (PDB code 2VT4[29]). The heavy atoms of the receptor binding site, as defined by residues within 5 Å from the ligand in the crystal structure, had an RMSD of 1.6 Å in the best model and a re-docked conformation of *S*-cyanopindolol had an RMSD of 0.5 Å.

The method was also used to generate a dopamine D_2 receptor homology model based on bovine rhodopsin (PDB code 1U19[120]), with the selective and rigid agonist *R*-NPA (**1**, **Figure 9**) present. Three loose distance restraints were set from two heavy atoms in the ligand (*meta* carbon in the catechol and the basic nitrogen) to three receptor atoms (in Asp114$^{3.32}$, Ser193$^{5.42}$ and Ser197$^{5.46}$) to roughly orient the ligand in the binding pocket. In addition, tethers were introduced between the Cα atom in those residues that were conserved between the model and the template. The strength of the tethers was

tuned such that computational resources were not spent on sparsely packed models (too weak restraints) while avoiding the regeneration of the starting structure (too strong restraints). The restraints were softened gradually during four geometry optimizing steps in the modeling procedure and in the final step they were turned off. In the initial step 472 complexes were optimized but the number of models was reduced stepwise by a score threshold based on geometry properties and energies. Despite the use of tethers during the initial step, the Cα RMSD was 3-12 Å, which demonstrates a wide sampling of the conformational space. The first optimizing step is fast and therefore the initial threshold was set to allow many receptor ligand complexes (38 models) to be evaluated in step two and three. After the second threshold nine complexes were selected for a final geometry optimization. These nine were further evaluated by docking a set of D_2 ligands, including actives and inactives, but the model had no discriminating ability.

The modeling approach is applicable also to other helical transmembrane proteins and is particularly useful when suitable protein templates are not available. This method development started when only few templates of GPCRs were available and it was therefore not used in the homology modeling of the dopamine receptors as several more relevant crystal structures had been published in the meantime.

3.2.2. Homology modeling of the dopamine D_2 receptor with agonist present (Paper II)

The recent crystal structures have contributed to an improved understanding of the GPCR structure and function. These findings have increased the possibilities for construction of more reliable homology models. It has been shown that docking in a homology model of drd3 gave similar result as docking in a crystal structure.[121]

A sequence alignment between the human adrenergic β_2 receptor (adrb2, 2RH1) and drd2 was performed using ClustalW (version 2.0.10).[122] The amino acid sequence for lysozyme in adrb2 and the third intracellular loop (IC3) in drd2 between TM5 and TM6 were both removed. The sequence alignment was carefully checked in less conserved regions close to the binding site and in loops. The second extracellular loop (EC2), which lines the binding site crevice, has shown to be important for agonist interaction and receptor activation.[93, 123] The loop includes a disulfide bridge (EC2-SS-TM3) that connects a cysteine residue in EC2 (Cys182) with a cysteine in TM3 ($Cys107^{3.25}$) (**Figure 15**), and constrains the loop on top of the crevice. Manual sequence alignment

adjustments were made in order to fill gaps in helices and to obtain the appropriate geometry of EC2. The most important modification in EC2 was the alignment of Ile184 and Asn186 close to the *N*-terminus of TM5, which have shown to be accessible for binding in drd2,[93] with the corresponding Phe and Thr residues which are pointing downwards into the binding crevice in the template structure (**Figure 15**).

The force field used for the receptor modeling in this study was Amber99[124] with R-field solvation, as implemented in the MOE software.[83] In the initial homology model, Pro187$^{5.36}$ at the *N*-terminus of TM5 was positioned in the EC2, although prolines are known to introduce kinks or terminate helices. To prevent Pro187$^{5.36}$ from being forced into the loop region, we used a novel strategy based on the introduction of an additional alanine residue just before the proline in EC2, which allowed proline to start the helix (marked with a green ring at the *N*-terminus of TM5 in **Figure 15**). The alanine residue was later manually deleted, which left a gap in the structure. The distance in the gap was reduced by a counterclockwise rotation around the center of the lower part of TM5 whereupon Pro187$^{5.36}$ and Asn186 could be connected. The sequence similarity between adrb2 and drd2 in the final manually adjusted alignment was 35% in total, 41% in the helix regions, and 57% in the binding pocket.

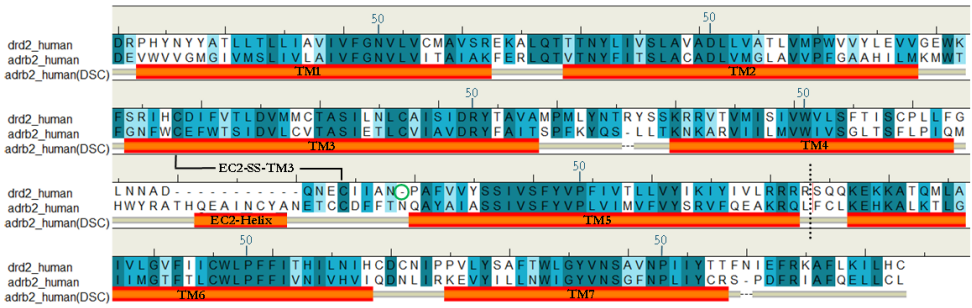

Figure 15. The final sequence alignment of the human adrenergic β_2 receptor (adrb2, 2RH1) and the human dopamine D_2 receptor (drd2). The adrb2 red bars (DSC) indicate the transmembrane (TM) helix regions and the second extracellular loop helix (EC2 Helix) in the adrb2 structure. The amino acid sequence for lysozyme in adrb2 and the third intracellular loop (IC3) in drd2 between TM5 and TM6 were excised, which is marked with a dashed line. The green ring at the *N*-terminus of TM5 indicates the gap where the alanine residue was introduced to prevent Pro188$^{5.37}$ from being forced into the EC2 (see text). Amino acids marked in dark blue indicate fully conserved positions, medium blue residues have highly similar physicochemical character, and light blue residues have less similar physicochemical character. The conserved cysteine bridge between TM3 and EC2 (EC2-SS-TM3) is indicated. The most conserved residue in each helix is marked with the index 50.

To collect more structural information regarding the agonist binding site in drd2 and the key interactions, the drd2 agonist *R*-2-OH-NPA[125] was present as environment in the binding site during the homology modeling procedure. *R*-2-OH-NPA is a structurally rigid full D_2 agonist that contains not only the typical D_2 agonist functional groups, such as a propyl-substituted basic amine and a catechol moiety, but also a hydroxy group in the 2-position (**Figure 16**). The reason for selecting this agonist was to make a stabilizing interaction possible between the ligand and Asn186 in EC2 via hydrogen bonding, in order to steer the Asn186 side chain towards the binding pocket.[93]

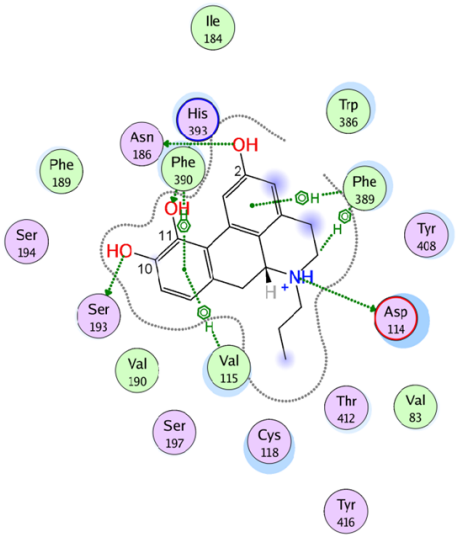

Figure 16. A schematic view of the interactions between the full agonist *R*-2-OH-NPA and the dopamine D_2 receptor homology model. The typical catecholamine agonist–receptor key interactions with Asp114$^{3.32}$ Ser193$^{5.42}$ and Phe390$^{6.52}$ are shown, together with the interactions between the hydroxyl group at the 11-position in *R*-2-OH-NPA and His393$^{6.55}$. In addition, the hydroxyl group at the 2-position participates in a hydrogen bond with Asn186 in EC2, and Phe389$^{6.51}$ forms a π–π interaction with the monohydroxylated phenyl group of the ligand. The characteristic propyl/allyl pocket is also indicated, located between the residues Val83$^{2.53}$, Cys118$^{3.36}$, Trp386$^{6.48}$, and Tyr416$^{7.43}$. Amino acids in purple are polar, while green residues are hydrophobic. The blue shades indicate ligand–receptor solvent accessibility.

During the modeling procedure, 20 homology models were generated independently, and for each model all side chain conformations were sampled three times. The backbone structure varied only little in the helical regions but considerably more in the loop regions, mainly in EC2 and IC2. The structural quality of the 60 homology models was evaluated carefully. The focus was directed at the agonist binding region and the important

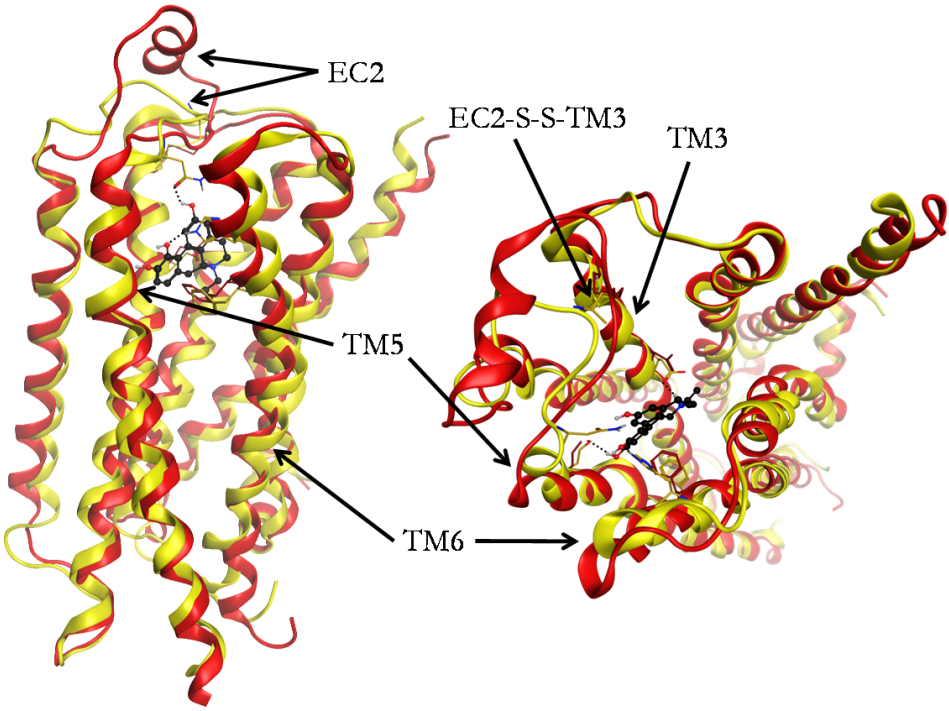

Figure 17. Two orthogonal views of the dopamine D_2 receptor (drd2) homology model (yellow) with the full agonist *R*-2-OH-NPA present in the binding site, and the structure of the adrenergic β_2 receptor (adrb2; 2RH1) in red. Some interacting amino acids of drd2 are included together with the corresponding residues in adrb2. These structures differ particularly in the second extracellular loop (EC2), but also in the upper part of transmembrane helix 5 (TM5) and TM6, where important interacting amino acids are positioned.

interacting amino acids (**Figure 16**). The following protein structural properties were inspected using the evaluation tools implemented in the MOE software:[83] 1) the bond lengths, angles and dihedrals of the protein backbone; 2) Ramachandran plots of φ-ψ dihedrals (general, glycine, proline, and pre-proline; for explanations, see **Figure A2** in Appendix); 3) side chain rotamer quality; and 4) non-bonded amino acid steric clashes.

To refine the model, hydrogen atoms were added to the ligand, and the ionization and tautomeric states of the ligand–receptor complex were determined. The selected complex was refined further by energy minimization with *R*-2-OH-NPA present in the binding site with motion restrictions on all heavy atoms. This step was followed by an unconstrained energy minimization. The overall geometry of the selected model was investigated and evaluated further with the more robust protein geometry evaluation program, Procheck.[85] According to Procheck the model had sufficiently good geometry,

with no residues in disallowed regions. The model had an RMSD value of 2.1 Å for all Cα atoms and 1.5 Å for the Cα atoms in the TM region, relative the template structure. Significant structural similarity was observed for the backbone except for the EC2, where the loop in the template adopts a helical structure (**Figure 15** and **Figure 17**). In addition, TM5 and TM6 were slightly tilted inward at the extracellular side, closing the binding pocket (**Figure 17**). The typical drd2 agonist key interactions were also present between 2-OH-*R*-NPA and the receptor (**Figure 16**). The distance from the oxygen atom in the C10 hydroxy group in 2-OH-*R*-NPA (the *para* position in its dopamine substructure) to the oxygen atom of the hydroxy group in Ser193$^{5.42}$ was 3.0 Å, and the O···H···O(Ser193$^{5.42}$) angle was 164º. Phe390$^{6.52}$ (II) was then positioned to make an optimal face to edge π-π-interaction with the aromatic catechol ring (I) in the ligand (r = 4.9 Å, θ = 88.1º and ω = 12.4º, see definition in **Figure 2**). On the opposite side of the catechol ring Val115$^{3.31}$ stabilized the position of the aromatic ring in the agonist via two C-H···π-interactions with a distance of 4.2 Å between the center of the aromatic ring and both Cγ atoms, which is sufficient for a good interaction.[16] The catechol oxygen atom of 2-OH-*R*-NPA that corresponds to the *meta* position in DA interacted with the imidazole NH group in His393$^{6.55}$ with a distance of 2.9 Å between the heavy atoms and an O···H-N(His393$^{6.55}$) angle of 157º (**Figure 16**). The other nitrogen atom of the imidazole ring in His393$^{6.55}$ interacted with the phenolic function in Tyr408$^{7.43}$ (**Figure 13**).

4. Dopamine D_1 agonist pharmacophore and receptor modeling

4.1. Dopamine D_1 agonist pharmacophore models and important amino acids for agonist binding

D_1 agonists have not been studied as much as D_2 agonists when it comes to pharmacophore modeling. Mottola et al.[126] have published a D_1 agonist pharmacophore model based on internal structural features such as the amino function and the oxygen atom of the *meta*-positioned hydroxy group in the catechol. This study also included a limited set of agonists together with a few inactive analogs, which were used to define forbidden volumes.

Like drd2 and all other catecholamine receptors, drd1 contains an aspartic acid residue in TM3 (Asp103$^{3.32}$), which forms a salt bridge with the basic amino group of the ligands.[46] Chemel et al.[127] and Pollock et al.[128] have shown that drd1 also includes a cluster of conserved serine residues (Ser198$^{5.42}$, 199$^{5.43}$, and 202$^{5.46}$) in TM5, of which Ser198$^{5.42}$ and Ser202$^{5.46}$ contribute most to the binding of the majority of agonists. SKF82958 (**23**), together with two analogs, also containing a chloride in the *meta*-position were however more sensitive to a Ser199$^{5.43}$→Ala than a Ser198$^{5.42}$→Ala mutation, and least affected by a Ser202$^{5.46}$→Ala mutation. The hydrophobic face, including Phe289$^{6.52}$, is highly conserved among the monomaminergic receptors and it could be expected that this residue is important for agonist binding as well as for activation also in the dopaminergic receptors.[51-53]

4.1.1. The construction of a new ligand based dopamine D_1 agonist pharmacophore model (Paper I)

The initial D_1 agonist pharmacophore model was constructed in a similar way as the D_2 agonist pharmacophore model, described above. A SEAL alignment of two low energy conformers of selective D_1 agonists (doxanthrine (**17**) ΔE = 0.0 kcal·mol^{-1} and SKF89626 (**21**) ΔE = 0.06 kcal·mol^{-1} **Figure 18** and **Figure 19a**) was the starting point. As drd1 and drd2 are relatively close homologs and have the key interacting amino acids in common, they also share the same type of pharmacophore features (Ser-TM5, Asp-TM3 and Aro). All known full drd1 agonists have a catechol function and in the initial pharmacophore

model two projected hydrogen bond acceptor/donor features (A- and B Ser-TM5) were included.

Full agonists

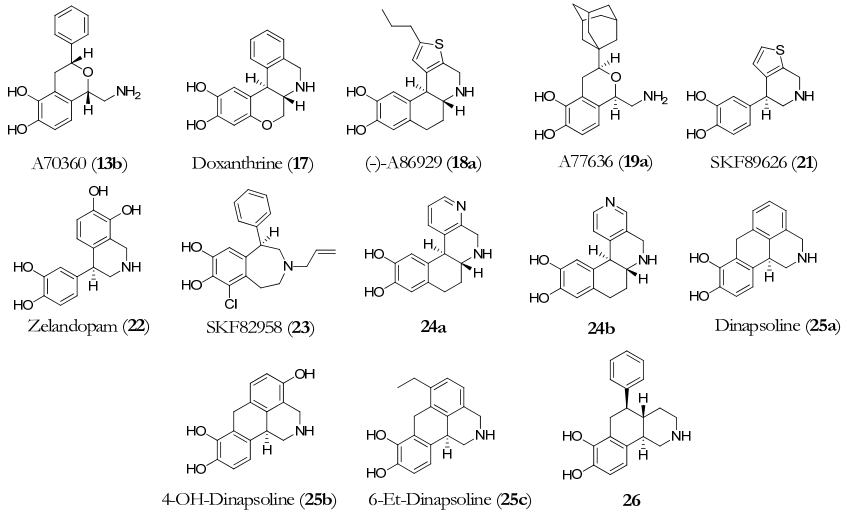

Partial agonists

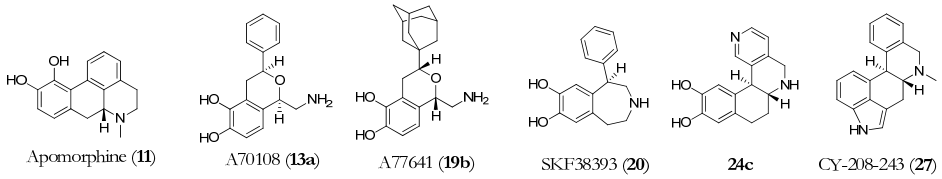

Inactives

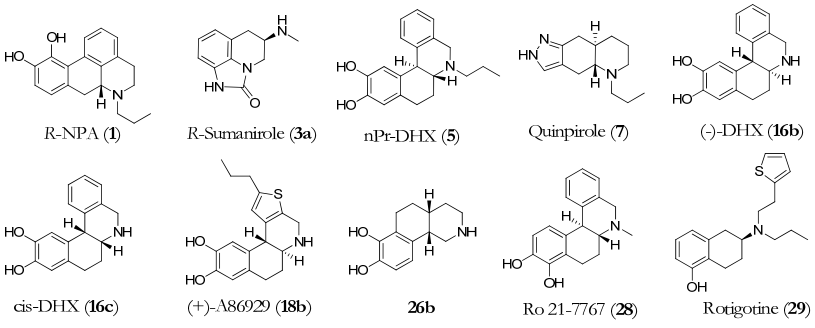

Figure 18. Selected full (**13b**, **17**, **18a**, **19a**, **21**, **22**, **23**, **24a-b**, **25a-c** and **26**) and partial (**11**, **13a**, **19b**, **20**, **24c** and **27**) D_1 receptor agonists and structurally related inactives (**1**, **3a**, **5**, **7**, **16b-c**, **18a**, **26b**, **28** and **29**).

As the main aim was to study D_2/D_1 agonist selectivity and the final D_2 agonist pharmacophore model only included a single Ser-TM5 feature, one of the features was removed from the D_1 agonist pharmacophore to prevent it from being a too strong determinant for the selectivity. In addition, a cation feature was introduced to guide the orientation of ligand hits (**Figure 19**). Thereby the D_1 pharmacophore model had the same composition and sizes of features as the D_2-model but the internal arrangement differed. The model was screened with a set of ligand conformations generated with conformational import, contained 12 full agonists, 6 partial agonist and 10 inactives and excluded volumes were introduced, in order to make the model selective. The final ligand based drd1 agonist pharmacophore model was screened against two conformational ensembles of D_1 ligands that were generated with both MMFF(S)[69] (MOE)[83] and OPLS_2005[70] (MacroModel)[80] force fields, using Born[72] solvation (water). It succeeded to include all but one full agonists (11/12, zelandopam (**22**) excluded), three of six partial agonists (3/6) and exclude all but three inactives (3/9), of the MMFFs generated ensemble of conformations. The screen of the OPLS_2005 generated conformations gave even better results (12/12, 4/6 and 1/9, **Table 2** and **Table A2**).

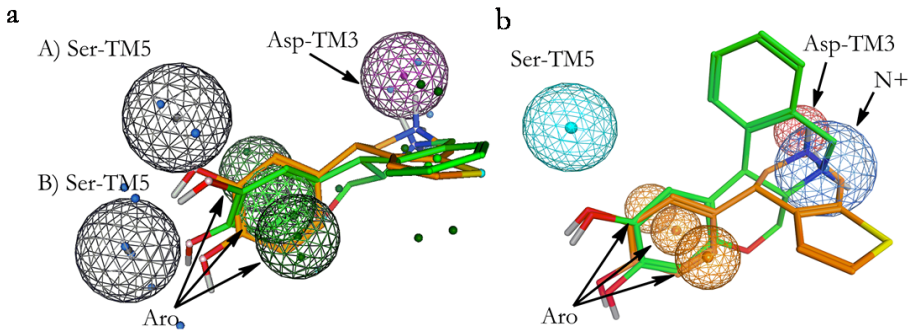

Figure 19. a) The initial dopamine D_1 agonist model (left) based on the superimposition of the full agonists doxanthrine (**17**; green) and SKF89626 (**21**; orange). The pharmacophore model consists of two projected hydrogen bond acceptor and donor features (Ser-TM5), a hydrogen bond donor feature that interacts with the protonated amino function (Asp-TM3), and a combined feature that defines the aromatic system (Aro). **b)** The final ligand and structure based D_1 agonist pharmacophore model which shares the feature arrangement with each other. The agonists **17** (green) and **21** (orange) are the pharmacophore hits in the structure based model (both ΔE=0.0 kcal·mol^{-1}). The two distinct binding modes are represented by the agonists. The excluded volumes are not shown in the picture.

4.1.2. The refinement of the dopamine D_1 agonist pharmacophore model guided by the receptor model (Paper III)

The selective D_1 agonist pharmacophore model was superimposed into a D_1 receptor structure model. A comparison was performed to see if the pharmacophoric features and excluded volumes were consistent with the shape of the binding pocket including interacting and sterically demanding residues (the receptor modeling details are described below in section *4.2.1.*). Unlike the drd2 agonist pharmacophore model the geometry of the feature arrangement was in good agreement with the interacting amino acids, but the excluded volumes had to be rearranged. Excluded volumes were introduced over the hydrogens with the van der Waals radii suggested by Bondi[106] as described for the D_2 model (i.e. 1.2 Å for aliphatic and 1.0 Å for aromatic, hydroxy, and amine [polar] hydrogen atoms). The sizes of the volumes were manually increased (1.5 and 1.3 Å) and the alignment of the feature part of the pharmacophore model in relation to the set of new excluded volumes was fine-tuned manually until the pharmacophore model was sufficiently discriminating. The excluded volumes (2.5 Å) covering the aromatic residues were introduced as in the D_2 model (**Figure 20**). The pharmacophoric feature arrangement was located even deeper into the receptor than the position of SKF89626 in the agonist/receptor complex (**Figure 20**). The position of the features was still in good agreement relative the key interacting amino acids (i.e., AspTM3, SerTM5 and Aro superimposed well with Asp103$^{3.32}$, Ser198$^{5.42}$, and Phe289$^{6.52}$, respectively, in the receptor model; **Figure 20**).

The set of D_1 ligands used to screen the previously described pharmacophore model, was supplemented with four novel compounds, three full agonists (4-OH- (**25b**) and 6-Et-dinapsoline (**25c**) and the octahydrobenzo[h]isoquinoline analog (**26**), and one inactive derivative (**26b**). The total number of screening ligands was fifteen full, six partial agonists and ten structurally similar inactives (**Figure 18**). The updated D_1 set was screened against the pharmacophore model and of the MMFF(S) generated ensemble all full agonists except zelandopam (**22**) (14/15), three out of six of the partial agonists (3/6, A77641 (**19b**), A70108 (**13a**) and CY-208-243 (**27**) did not hit) and four out of nine of the inactives (4/9; (-)-DHX (**16b**), rotigotine (**29**), *R*-NPA (**1**) and *n*Pr-DHX (**5**)) hit the pharmacophore. The screen of OPLS-2005 generated conformers turned out to be

slightly better, where two more inactives were discriminated ((-)-DHX (**16b**) and *R*-NPA (**1**)) and one more partial agonist hit the pharmacophore (A70360 (**13b**)). A difference was also that A70360 (**13b**) hit the model but not zelandopam (**22**). The reason why **13b** and its enantiomer **13a** are on the border of matching the pharmacophore model may be reflected by the fact that **13b** is a full agonist, but with only low affinity, whereas its enantiomer **13a** is a potent partial agonist (IA~60%).[129]

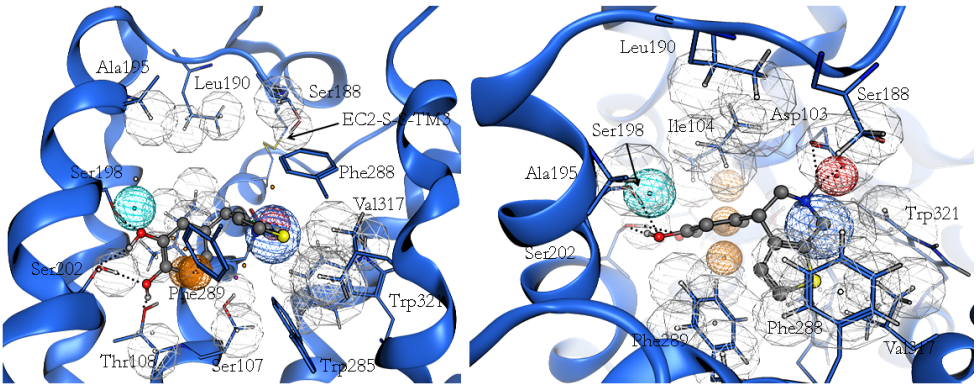

Figure 20. Side (left) and top view (right) of the receptor-based pharmacophore model superimposed onto the D_1 structure model. The backbone ribbon for TM6 and the corresponding excluded volumes are not shown. The conformation of SKF89626 is taken from the ligand–receptor model complex, while the relative positions of the pharmacophore features are tuned to generate the best hit rate.

The ligand set contains one full agonist with an *N*-substituent (SKF82958, **23**), but unlike the other full agonists it contains also a chloride in the *meta*-position in the catechol ring. In the pharmacophore hit of **23** the chloride pointed towards the backbone carbonyl oxygen of Ser107$^{3.36}$ (distance 2.7 Å and C-Cl···O-angle 153º). The analog lacking the Cl-substituent had five times lower affinity for drd1 and showed also lower intrinsic activity.[130] The increased affinity of **23** indicates that the chloride is likely to be involved in a specific intermolecular interaction with a geometry well corresponding to a halogen bond.[131] This is in agreement with findings from mutations studies by Pollock at el.[128] and Chemel et al.[127] who showed that **23** is relatively insensitive to a Ser202$^{5.43}$→Ala mutation and moderately affected by a Ser199$^{5.43}$→Ala mutation. This halogen bonding may compensate for Ser-TM5 interactions and allow a deeper binding mode of **23** which might be required for full efficacy.

Table 2. Results of the ligand and structure guided D_1 agonist pharmacophore models search of two different ensembles of generated conformations.

Ligand		Structure guided pharmacophore model						Ligand based pharmacophore model					
		MOE stochastic search Born solvation, MMFF94(S)[a]			*MacroModel serial torsion search GB/SA solvation, OPLS2005*[b]			*MOE stochastic search Born solvation, MMFF94(S)*[a]			*MacroModel serial torsion search GB/SA solvation, OPLS2005*[b]		
		ΔE[c]	RMSD[d]	#c/#h[e]	ΔE[c]	RMSD[d]	#c/#h[e]	ΔE[c]	RMSD[d]	#c/#h[e]	ΔE[c]	RMSD[b]	#c/#h[e]
Dopamine (**12**)	Full	0.0	0.66	6/1	0.0	0.64	20/8	0.0	0.66	6/1	0.0	0.64	20/8
A70360 (**13b**)	Full	1.5	0.65	7/1			13/0	0.0	0.67	7/5	2.1	0.67	13/5
DHX (**16a**)	Full	0.8	0.63	2/1	0.0	0.13	14/14	0.0	0.23	2/1	0.0	0.13	14/8
Doxanthrine (**17**)	Full	0.5	0.60	2/1	0.0	0.11	14/14	0.0	0.12	2/2	0.0	0.11	14/6
(-)-A86929 (**18a**)	Full	0.0	0.54	10/6	0.0	0.52	73/58	0.0	0.54	10/10	0.5	0.12	73/36
A77636 (**19a**)	Full	1.4	0.30	3/1	0.0	0.26	11/7	0.0	0.28	3/2	0.0	0.26	11/7
SKF89626 (**21**)	Full	0.1	0.61	4/2	0.0	0.63	20/6	0.1	0.61	4/2	0.0	0.63	20/6
Zelandopam (**22**)	Full			4/0	0.0	0.63	40/13			4/0	2.9	0.63	40/2
SKF82958[d] (**23**)	Full	3.8	0.47	22/1	2.2	0.40	50/6	1.8	0.41	22/1	0.0	0.43	50/8
24a	Full	1.6	0.59	2/1	1.6	0.61	6/2	0.0	0.22	2/2	0.0	0.13	6/4
24b	Full	0.0	0.23	2/2	0.2	0.62	12/6	0.0	0.23	2/2	0.0	0.12	12/6
Dinapsoline (**25a**)	Full	0.0	0.39	1/1	0.0	0.45	4/4	0.0	0.39	1/1	0.0	0.45	6/4
4-OH-Dinapsoline[g] (**25b**)	Full	0.0	0.36	1/1	0.0	0.46	8/5						
6-Et-Dinapsoline[g] (**25c**)	Full	0.0	0.37	6/3	0.0	0.46	16/16						
26[g]	Full	0.0	0.55	2/2	0.0	0.56	16/8						
Apomorphine (**11**)	Partial	0.0	0.61	2/1	0.0	0.62	4/2	0.0	0.61	2/1	0.0	0.62	4/2
A70108 (**13a**)	Partial			6/0	0.0	0.56	11/7	0.0	0.71	6/3	0.0	0.72	11/7
A77641 (**19b**)	Partial			3/0			11/0			3/0	2.8	0.67	11/2
SKF38393 (**20**)	Partial	0.4	0.68	5/2	0.0	0.47	20/16	0.0	0.43	5/3	0.0	0.62	20/10
24c	Partial	0.0	0.62	2/2	0.9	0.61	8/4			2/0			8/0
CY-208-243 (**27**)	Partial			3/0			1/0			3/0			1/0
R-NPA[d] (**1**)	Inactive	2.5	0.60	6/1			27/0			6/0			27/0
S-Sumanirole (**3a**)	Inactive			5/0			4/0			5/0			4/0
nPr-DHX[d] (**5**)	Inactive	1.3	0.42	17/2	3.4	0.43	56/2			17/0			56/0
Quinpirole (**7**)	Inactive			4/0			9/0			4/0			9/0
cis-DHX (**16c**)	Inactive			5/0			12/0	2.7	0.62	5/1	3.4	0.62	12/4
(-)-DHX (**16b**)	Inactive	0.8	0.74	2/1			8/0	0.8	0.74	2/1			8/0
(+)-A86929 (**18b**)	Inactive			10/0			41/0			10/0			41/0
26b	Inactive			2/0			8/0						
Ro 21-7767[d] (**28**)	Inactive			4/0			8/0			4/0			8/0
Rotigotine[d] (**29**)	Inactive	1.3	0.73	186/5	1.9	0.72	486/13	3.6	0.69	186/2			486/0

[a] The energy cutoff for conformations generated in MOE is 4 kcal mol^{-1}. [b] The energy cutoff for conformations generated in MacroModel is 16.7 kJmol^{-1} (~4 kcal mol^{-1}). [c] The lowest relative energy [kcal mol^{-1}], with respect to the most stable conformer in the ensemble, for the conformers that fit the pharmacophore model. [d] Root of the mean square distance between the center of the pharmacophore features and their matching ligand annotation points. [e] #c: number of conformations generated for the respective method; #h: number of conformations that hit the pharmacophore model. [f] The amine is tertiary and therefore considered chiral, and two different configurations have been used in the modeling. [g] The compounds are new in this study and therefore were not screened against the previously published pharmacophore model.

4.2 Dopamine D_1 receptor structure modeling

4.2.1 Homology modeling of the dopamine D_1 receptor with agonist present (Paper III)

A drd1 model was constructed in the same way as described above for the drd2 (section *3.2.2*). A multiple sequence alignment using the human adrenergic β2 receptor (adrb2, PDB code: 2RH1), drd1, and drd2 was performed using ClustalW[122] (Appendix **Figure A1**). Some manual adjustments were done in order to fill gaps in the sequences and an amino acid stretch (WYRAT) in EC2 was cut out in the template structure in order to let the program freely predict the 3D structure for the considerably longer stretch in drd1. The sequence similarity between adrb2 and drd1 in the manually adjusted alignment was 36% in total, 43% in the TM helix region, and 67% in the binding pocket (the corresponding sequence similarity between drd1 and drd2 is 34, 43, and 55%, respectively).

Figure 21. The refined multiple sequence alignment of the human adrenergic β2 receptor (adrb2, 2RH1) and the dopamine D_1 (drd1) and D_2 (drd2) receptors. The adrb2 (DSC) bars indicate the transmembrane (TM) helix regions and the helix in the second extracellular loop (EC2 Helix) in the adrb2 structure. The lysozyme in adrb2 and the third intracellular loop (IC3) in drd1 and drd2 between TM5 and TM6 were excised; this is indicated with a dashed line. The strikethrough amino acid stretch WYRAT was cut out in the template structure. The green ring at the *N*-terminus of TM5 in the drd2 sequence indicates the gap caused by the smaller number of amino acids between the cysteine bridge (EC2-SS-TM3) and TM5. Amino acids marked in dark blue indicate fully conserved positions, medium blue residues have highly similar physicochemical character, and light blue residues have less similar physicochemical character. The conserved cysteine bridge between TM3 and EC2 (EC2-SS-TM3) is indicated. The most conserved residue in each helix is marked with the index 50.

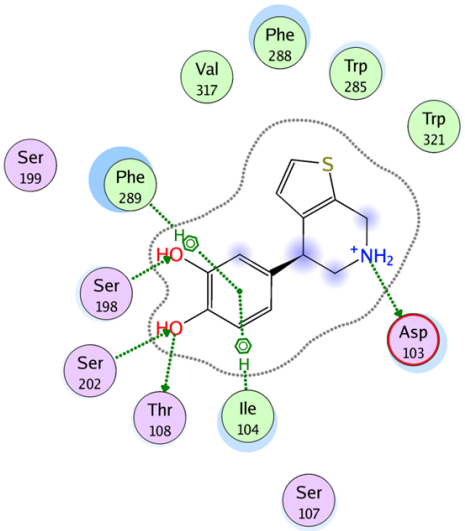

Figure 22. A schematic view of the interactions between the full agonist SKF89626 (**21**) and the dopamine D_1 receptor homology model. The typical catecholamine agonist–receptor key interactions with Asp103$^{3.32}$, Ser198$^{5.42}$ and Ser202$^{5.46}$ are shown. The *meta*-hydroxy group of SKF89626 interacts via hydrogen bonding with Ser198$^{5.42}$ and the *para*-hydroxy group interacts with Ser202$^{5.46}$. The *para*-hydroxy group also forms a hydrogen bond to Thr108$^{3.37}$, while the aromatic ring in the agonist forms a face-to-edge π–π interaction with Phe289$^{6.52}$ and a methyl–π interaction with Ile104$^{3.33}$. Polar residues are shown in purple, whereas hydrophobic residues are in green. Blue shades indicate ligand–receptor solvent accessibility.

The potent and full D_1 agonist (+)-doxanthrine[132] (DOX, **17**) was present in the binding site during the generation of the homology models. DOX is a chromane-based analog of DHX, but unlike DHX, it is selective for D_1 receptors.[132] A total number of 60 drd1 models were generated and in these models the backbone differed considerably in the *C*-terminal part of TM4, in the EC2 close to the disulfide bridge, and around the IC1 loop, but particularly in EC3. The conformations of the side chains varied also in these regions. Such differences were also observed in helical regions where more than one optimal packing solution is possible. The force field used for the receptor modeling was Amber99[124] with R-field solvation, as implemented in the MOE software.[83] The two ligands, SKF89626 (**21**, **Figure 20** and **Figure 22**) a super-agonist (**Figure 3**) with an intrinsic activity of 120%[133-134] and zelandopam[135] (**22**, **Figure 18**) have similar scaffolds, in which the catechol ring is linked via a single bond to a bicyclic motif. As mentioned above, all full D_1 agonists contain a catechol function, and when aligning these aromatic rings, the binding mode of **21** and **22** differ from the remaining set of agonists. The low-

energy conformations of **21** and **22** have the bicyclic motif oriented perpendicular to the catechol and the receptor aligned pharmacophore hits would therefore clash into residues in TM6. Therefore, it was concluded that D_1 agonists may bind in two distinct binding modes when the structure guided excluded volumes have been introduced (**Figure 19**). The modeling approach which is based on an iterative procedure including both structure and ligand based methods made this observation possible.

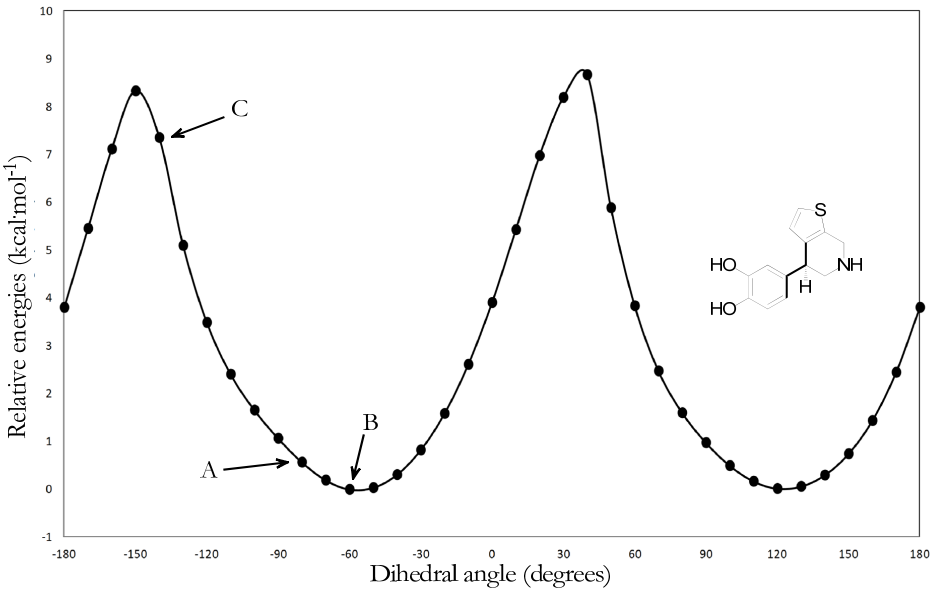

Figure 23. The dihedral angle energy profile for the bond connecting the two ring systems in SKF89626. The dihedral angle in the ligand is marked in bold. A) The conformation of SKF89626 in the ligand/receptor complex with a relative energy of ~0.6 kcal·mol^{-1}. B) The global minimum. C) The conformer of SKF89626 just after the planarity flip.

When evaluating the rotational energy of the dihedral angle between the ring systems in **21**, we found that the energy barrier to planarity was **~**8 kcal mol^{-1} (**Figure 23**). In addition, dinapsoline (**25a**, **Figure 18**) also had steric clashes in this region which particularly involved Phe288$^{6.51}$. Therefore, different side chain rotamers of Phe288$^{6.51}$ were evaluated to create space for **25a**, **21**, and **22**. A more favorable rotamer of phenylalanine was selected and DOX was replaced by **21** in the binding site. A subsequent energy minimization was performed, which resulted in the movement of Val317$^{7.39}$ in between Phe288$^{6.51}$ and Trp285$^{6.48}$ to form a larger cavity for these three agonists. This modification of the model did not affect the binding mode of DOX and the typical

monoaminergic key interactions, i.e. the ionic interaction to Asp103$^{3.32}$, the hydrogen bonds to the serine residues (Ser198$^{5.42}$ and Ser202$^{5.46}$) and the face-to-edge π-π interaction with Phe289$^{6.52}$, were still present in the D_1 receptor–agonist complexes (**Figure 22**).

The basic amino group of the ligand interacted almost symmetrically with both oxygen atoms in Asp103$^{3.32}$ and formed salt bridges with N-O distances of 2.7 and 2.9 Å, and N-H···O(Asp103$^{3.32}$) angles of 158º and 130º. The other hydrogen atom in the amino function of **21** was just outside the defined distance to form a hydrogen bond with Ser107$^{3.36}$ (d=4.6 Å, angle=175º). The hydroxyl group of Ser107$^{3.36}$ was directed toward the binding crevice and interacted with the backbone carbonyl of Asp103$^{3.32}$, this residue has shown to be important for agonist binding in both the drd1[136] and 5-HT_{2A}[137] receptors. The distance from the oxygen atom in the *para*-hydroxy group of **21** to the oxygen in the hydroxyl group of Ser202$^{5.46}$ was 2.7 Å and the O···H···O(Ser202$^{5.46}$) angle 178º. In addition, the *para*-hydroxy group interacted also via a hydrogen bond to Thr108$^{3.37}$ (d=2.7 Å, a=176º). The oxygen atom of the *meta*-hydroxyl interacted instead with Ser198$^{5.42}$ with a distance of 2.8 Å between the heavy atoms and an O···H···O(Ser198$^{5.42}$) angle of 166º. The hydroxyl-oxygen in Ser199$^{5.43}$ was 4.6 Å away from the oxygen in the *meta*-hydroxy group of **21** and could therefore not interact directly with the ligand, but interacted instead via a hydrogen bond to Asn292$^{6.55}$. This was in agreement with the findings by Chemel and co-workers,[127] who suggested that the binding of the majority of the D_1 agonists in their study were least sensitive for a Ser199$^{5.43}$→Ala mutation.

The phenylalanine residue, Phe289$^{6.52}$ (II), which has proven to be important for agonist binding and activation of GPCRs,[51, 54] was positioned to form a face-to-edge π-π interaction with the catechol ring of SKF89626 (**21**) (I), but the angles were just on the border of being appropriate (r = 4.9 Å, θ = 74.0º and ω = 17º, see definition in **Figure 2**). As in the drd2-agonist complex, the aromatic catechol of **21** was stabilized from the opposite side of Phe289$^{6.52}$, via C-H···π-interactions from Ile104$^{3.33}$. The distance between the center of the aromatic ring and the Cγ atoms were 4.1 and 4.2 Å and the angles 145º and 152º (Cγ-H···centroid), respectively, which is sufficient for a good interaction.[16] The position of the thiophene moiety of SKF89626 was stabilized by the

aromatic/hydrophobic cluster in TM6 and TM7, which includes residues Phe288$^{6.51}$, Phe289$^{6.52}$, Trp285$^{6.48}$, Val317$^{7.39}$, and Trp321$^{7.43}$ (**Figure 22**). In EC2, which has been found to be important for agonist binding and activation of GPCRs,[93, 123] two amino acids (Ser188 and Leu190) were directed downwards into the binding site crevice and can thus make additional interactions with the ligand.

The refined SKF89626-minimized D_1 receptor model had an RMSD relative to the template structure (2RH1) of 2.8 Å for Cα and 1.94 Å for Cα in the TM-region. The generated structure model showed good geometric quality according to the evaluation tools implemented in MOE[83] (Ramanchandran plots are shown in Apendix, **Figure A3**). The model was further investigated with the Procheck program,[85] which showed that with the exclusion of glycines and prolines, 86% of the residues belonged to the most favored region of the Ramachandran map, 16% in the allowed, and 1% in the generously allowed region. No residues belonged to disallowed regions and all main chain and side chain geometries were designated to the "better" class. Close contacts were identified, all represented by protein ligand interactions.

5. Dopamine D_2/D_1 agonist selectivity

5.1. Comparison of dopamine D_2 and D_1 agonist models

The D_1 homology model had an RMSD in relation to the corresponding D_2 model of 2.2 Å for Cα and 1.4 Å for Cα in the TM region. Thus, the dopamine receptor models were more similar to each other in the TM region than they were to the template structure (drd1–adrb2: 2.8 Å for all Cα and 1.9 Å for Cα in the TM region; drd2–adrb2: 2.1 Å for all Cα and 1.5 Å for Cα in the TM region). An overlay of the two models is shown in **Figure 24**. The orthosteric binding pockets, defined as amino acids within 3.5 Å of the corresponding agonists, were located between TM2, 3, 5, 6, and 7, and the EC2 lines the top of the binding crevice. The volume of the binding pocket of drd2 is 371 $Å^3$, whereas it is considerably larger (495 $Å^3$) for drd1. The radii of the optimized excluded volumes of the drd1 agonist pharmacophore models were 1.5 Å for aliphatic and 1.3 Å for aromatic and polar hydrogen atoms in drd1, and 2.1 and 1.9 Å, respectively, in drd2. This indicates that the models probably underestimate the actual size difference between the receptor binding sites.

The optimized positions of features in the drd1 pharmacophore model were shifted downward, corresponding to a deeper binding mode in the receptor relative to the feature arrangement in the D_2 pharmacophore model.

The binding pockets for both receptors have 22 amino acids in common, all within 3.5 Å from the ligands. Of these are ten positions non-conserved and could be expected to have strong influence on agonist selectivity. Drd1 has a serine residue (Ser107$^{3.36}$) one turn down in the membrane relative to the Asp$^{3.32}$, which interacts with the backbone carbonyl of the aspartate residue. In drd2 there is a cysteine residue in the corresponding position which has a conformation that points out in the crevice and prevents lower binding modes. In addition, the cysteine residue has an inferior hydrogen bonding capacity to that of serine, which makes hydrophilic elements less favorable in D_2 ligands. This fact can explain the difference in selectivity between the drd2 selective agonist DHX (**16a**) and its analog DOX (**17**), which is a selective potent D_1 agonist. The latter contains an ether function that points toward Ser/Cys$^{3.36}$. An additional indication that DOX most

likely interacts with Ser107$^{3.36}$ is that DHX, which cannot make this TM3 interaction is more affected by the Ser-TM5 mutations than DOX.[127] Unlike the majority of selective D_2 agonists, the D_1 agonists contain a primary or secondary amine which is able to form an additional hydrogen bond to Ser107$^{3.36}$ beyond that to the aspartate.

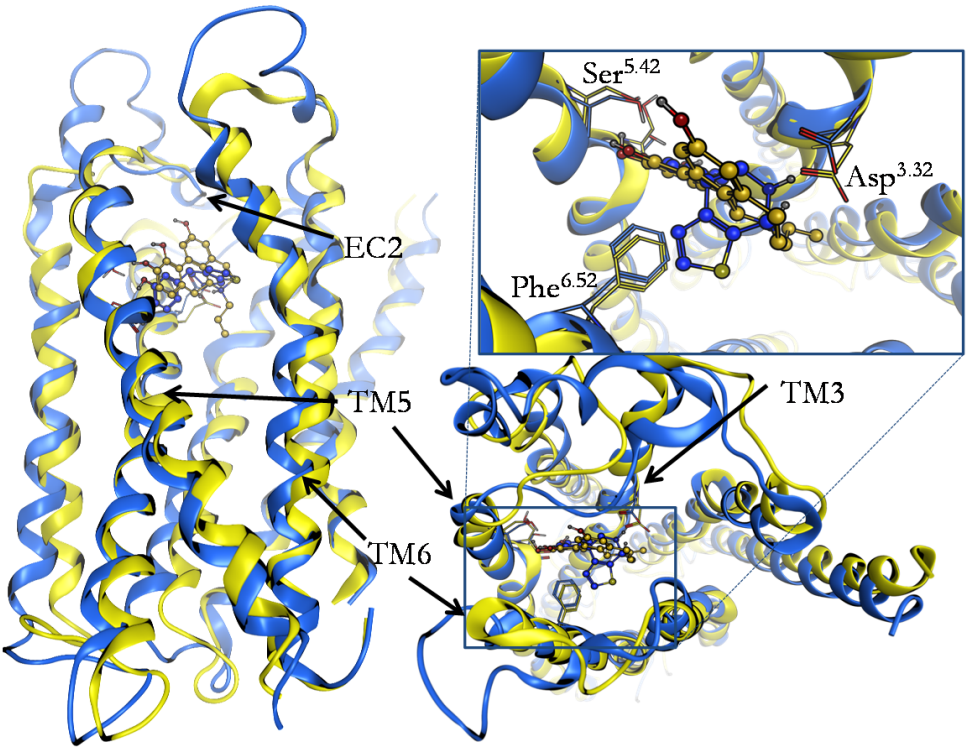

Figure 24. Two orthogonal views of the superimposed dopamine D_1 (blue) and D_2 (yellow) receptor models together with the corresponding full agonists *R*-2-OH-NPA (blue) and SKF89626 (**21**, yellow) present in their binding sites. The typical monoaminergic key interacting amino acid residues are shown explicitly. The structures differ particularly in the second and the third extracellular loops (EC2 and EC3), but also in the transmembrane (TM) region, where important interacting amino acids are positioned.

Of special interest were the interactions made by the DHX diaza-analogues **24a-c** (**Figure 18**) to residues in EC2 of drd1. The aromatic nitrogen atom in the most potent and full D_1 agonist 4,6-diaza analog **24a** may form a hydrogen bond with Ser188 in EC2 (**Figure 25**). The distance between the heavy atoms in the hydrogen bond was 4.3 Å and the N···H-O(Ser188) angle was 139º, a distance and angle considered to be suboptimal for a hydrogen bond. However, Ser188 could most likely change its conformation to a

position more available for hydrogen bonding, due to its location in the flexible loop. The 3,6-diaza analog **24b**, showed slightly lower affinity than **24a**, but had full efficacy for the D_1 receptor. Finally, the 2,6-diaza analog **24c** has even lower affinity and also lower efficacy. In the pharmacophore hits of **24c**, the nitrogen atom points toward the hydrophobic Leu190 residue located in EC2. Interestingly, **24c** was the most potent analog at the drd2 with a similar affinity as DHX.[138] The corresponding residue to Leu190 in drd2 is an asparagine (Asn186), whereas the Ser188 in drd1 corresponds to Ile184, which may reflect the D_1/D_2 binding selectivity of the diaza-analog. This result was in analogy with the potent and full intrinsic dinapsoline analogs **25b** and **25c**,[139] where **25b** has a hydroxyl function pointing towards Ser188 and **25c** an ethyl substituent pointing in the direction of Leu190 in drd1.

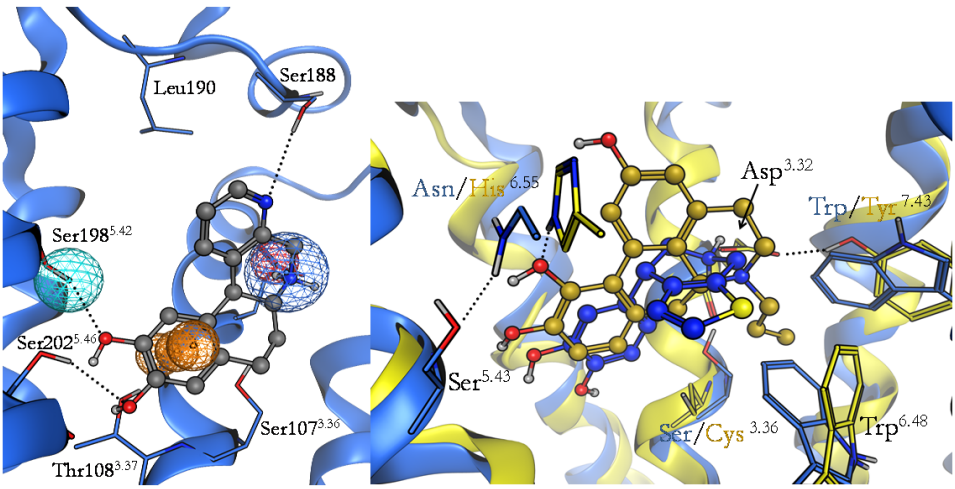

Figure 25. Left: The pharmacophore hit of the 4,6-diaza analog **24a** which forms a hydrogen bond with Ser188 in EC2 in the D_1 receptor model. The distance between the heavy atoms in the hydrogen bond is 4.3 Å and the angle (N···H-O(Ser188)) is 139°. Right: A side view of the superposed drd1 (blue) and drd2 (yellow) models. TM6 is cut out. The conserved tryptophan residue in TM6 that differs in conformation and forms the D_2-characteristic propyl pocket together with amino acids in TM2, TM3, and TM7, Trp$^{6.48}$. Tyr$^{7.43}$ in drd2 interacts with Asp$^{3.32}$, whereas the corresponding residue (Trp$^{7.43}$) is unable to make that bond and is instead rotated toward TM6 and Trp$^{6.48}$. His$^{6.55}$ interacts with the *meta*-hydroxy group of the D_2 agonist *R*-2-OH-NPA (yellow), while the corresponding Asn$^{6.55}$ forms a hydrogen bond with Ser$^{5.43}$. The D_1 agonist SKF89626 (blue) binds deeper in the binding crevice.

The TM5 serine residues that are part of the binding site are conserved between drd1 and drd2. TM5 in the drd2 model is rotated slightly inward toward the ligand binding site relative to the drd1 model, which makes the serine residues in drd2 less optimally

positioned for catechol interaction. This was also reflected in the D_2 agonist pharmacophore model, for which the hit rate was the same when the priority of the Ser-TM5 feature was redefined from essential to optional. This was in contrast to the D_1 pharmacophore model where the essentiality for Ser-TM5 feature hits was crucial.

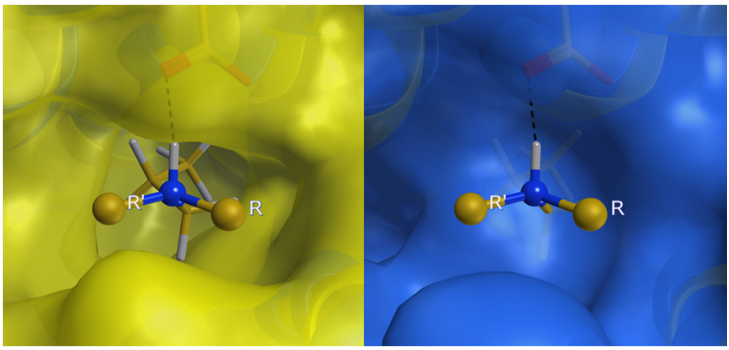

Figure 26. Representation of the solvent-accessible surface of the D_2 (left) and D_1 (right) receptors, as viewed from the binding pocket in the direction of the D_2-characteristic propyl pocket region. The *N*-propyl functional group of *R*-2-OH-NPA is included to illustrate the shape difference between the receptors in that region.

The hydrophobic face in TM6 is highly conserved between receptors, but they differ in position 6.55, where drd2 has a histidine and drd1 an asparagine residue. In mutagenesis studies His393$^{6.55}$ has been shown to be involved in agonist binding in drd2,[92] unfortunately the corresponding Asn292$^{6.55}$ in drd1 has not been studied. The asparagine residue is conserved in relation to the template structure (Asn293$^{6.55}$) and has shown to be involved in agonist binding in adrb2.[140] In the drd2 model His393$^{6.55}$ was accessible for ligand interaction, whereas Asn292$^{6.55}$ in drd1 was rotated toward TM5 and instead interacted with Ser199$^{5.43}$ (**Figure 25**). The additional polar interaction between the ligand and His393$^{6.55}$ in drd2 may explain D_2 agonism of ligands with aromatic hydrogen bonding substituents other than the catechol function. Furthermore, D_1 agonists cannot make polar interactions with residues in TM6, and for that a catechol function seems to be optimal for the Ser-TM5 interactions. The phenylalanine residue (Phe$^{6.52}$), which forms a face-to-edge π–π interaction with the agonists, was positioned almost identically in the two models. The rotamers of the tryptophan residue (Trp$^{6.48}$) one turn down in the membrane relative Phe$^{6.51}$, differ to some extent between the receptors. Trp386$^{6.48}$ in drd2 adopted a conformation where the side chain was directed toward TM7, while the

corresponding tryptophan in drd1 was sterically hindered by the non-conserved Trp321$^{7.43}$, which was rotated out towards the ligand binding site (**Figure 25**). In the drd2, Tyr416$^{7.43}$ interacts with Asp114$^{3.32}$ and was anchored up towards TM2, which opened up the cavity referred to as the propyl pocket, localized between the residues Val83$^{2.53}$, Cys118$^{3.36}$, Trp386$^{6.48}$, Thr412$^{7.39}$, and Tyr416$^{7.43}$ (**Figure 16** and **Figure 26**) This cavity was not present in the drd1 model (**Figure 25** and **Figure 26**). These geometrical differences in TM6 and TM7 between D_1 and D_2 might be a second reason why *N*-substituents are present on D_2 but not on D_1 agonists. It could also explain the diverse binding modes of the D_1 agonists.

6. Concluding remarks

We have developed selective D_2 and D_1 agonist pharmacophore models by using a strategy based on projected features and excluded volumes. To generate robust and truly discriminating 3D pharmacophore models, it was important that the set of actives used to build the models were structurally diverse and conformationally rigid. In addition, closely structurally related inactive analogs were needed. Therefore sets of well-characterized full agonists and inactives were carefully selected from the literature. The inactives were either agonists selective for the other receptor, inverse agonists, antagonists, or true inactives.

We also constructed dopamine D_2 and D_1 receptor 3D models with an agonists present in the binding site during the modeling procedure in order to steer the receptor towards the agonist bound states. The generated selective pharmacophore models were superimposed into their corresponding receptor model, and the pharmacophores were further refined based on information from the 3D receptor models and published experimental data. These pharmacophore models included forbidden areas where no matching heavy atoms are allowed, in order to reflect the shape of the binding pocket. The combination of receptor and pharmacophore modeling gave a unique possibility to identify key factors for D_2 /D_1 selectivity, such as:

- The Ser-TM5 interactions are not as important for D_2 as for D_1 agonists
- The binding mode for D_1 agonists seems to be deeper in the binding pocket than for D_2 agonists
- The sizes of the excluded volumes indicate that the binding pocket in the drd1 homology model is too narrow
- The unconserved Ser107$^{3.36}$ residue in TM3 is important for D_1 agonist binding
- Interactions with EC2 are important for agonists to both receptors, but are of different nature
- The unconserved His393$^{6.55}$ residue in TM6 is important for D_2 agonist binding
- The unconserved Trp/Tyr$^{7.43}$ residue in TM7 contributes to the formation of the drd2-specific propyl pocket, where Tyr416$^{7.43}$ interacts with Asp114$^{3.32}$ and opens up the cavity

A semi-empirical helix docking approach was developed for modeling of helix containing receptor targets (GPCRs and other transmembrane helix proteins). The method was used to build models of both the β_1-receptor and the D_2 receptor. A docking study using the latter showed however that the model was not selective as it did not only accommodate all full agonists but also most of the structurally related inactives.

The use of a combination of computational methods together with information from available experimental findings gives the opportunity to generate more reliable and predictive models. The approach described in this thesis is considered to be general and therefore applicable to many other systems. It is especially useful in less well-characterized systems to explore ligand–receptor interactions and to guide the construction of each model to make it more credible for further analysis.

7. Acknowledgement

Jag vill passa på att tacka alla som bidragit med ideér, hjälp och stöd under min tid som doktorand.

Först och främst vill jag tacka **Kristina Luthman**, min handledare för att du antog mig som doktorand och för att du generöst delat med dig av dina vetenskapliga erfarenheter och idéer. Du har varit ett enormt stort stöd under hela denna tid och jag hade inte kunnat ha en bättre handledare!

Min andra huvudhandledare **Peder Svensson** för all hjälp med handledning och allt annat och för att du är en så god vän!

Min biträdande handledare **Lars Brive**, för att du delat med er av era värdefulla kunskaper inom vetenskapen. Jag vill också tacka Lars examensarbetare **Ronnie Persson** för utmärkt arbete med helix-dockningsmetoden.

Mina examinatorer **Ann-Therese Karlberg** och senare, **Johan Gottfries** för givande samtal.

Min enda, men helt ok examensarbetare, **Ivana Uzelac.**

Ni som jag fått diskutera modellering med på våning 8: **Jürgen**, **Peter D**, **Per-Ola**, **Sten**, **Fredrik W** och **Johan G**.

Nicholas Waters och **Clas Sonesson**, för att jag fick möjlighet att vara på NeuroSearch och för givande diskussioner om dopamin.

Alla andra på NeuroSearch för alla trevliga stunder

Alla ni som hjälpt till med fix och trix med avhandling, och att korrekturläsa den. **Itedale**, **Maria**, **Mariell**, **Tobias**, **Mate**, **Jürgen, Johan G**, **Peder** och **Kristina**.

Vännerna i matlaget med **David**, **Jenny**, **Emma**, **Mariell** och **Tobias**, för god mat och goda samtal.

Alla mina vänner i Göteborg, i övriga Sverige och övriga världen.

Alla studiekamrater genom åren.

Alla människor på vån 8 och 9.

Min familj, med Mamma **Eva,** mina bröder **Magnus** och **Martin**, med familjer, och all övrig släkt.

Sist men inte minst, min älskade **Julia** och vår underbara dotter, **Majken!**

8. Appendices

Table 1. Results of the D_2 agonist pharmacophore search of the four different ensembles of generated conformations.

Ligand		*MOE conformational import Born solvation, MMFF94(S)*[e]			*MOE stochastic search Born solvation, MMFF94(S)*[e]			*MacroModel serial torsion search GB/SA solvation, MMFF(S)*[f]			*MacroModel serial torsion search GB/SA solvation, OPLS2005*[f]		
		ΔE[a]	RMSD[b]	#c/#h[c]	ΔE[a]	RMSD[b]	#/#h[c]	ΔE[a]	RMSD[b]	#c/#h[c]	ΔE[a]	RMSD[b]	#c/#[c]
R-NPA (**1**)[d]	Full	0.0	0.61	10/6	0.0	0.59	12/6	0.0	0.58	16/16	0.0	0.45	21/19
Talipexole (**2**)[d]	Full	0.0	0.50	48/21	0.0	0.54	44/22	0.0	0.51	44/22	0.0	0.51	28/14
R-Sumanirole (**3a**)	Full	0.0	0.26	5/2	0.0	0.32	5/2	0.0	0.26	5/2	0.0	0.23	3/2
RR-PHNO (**4a**)	Full	0.0	0.47	9/6	0.0	0.51	6/4	0.0	0.51	17/17	0.0	0.50	12/12
nPr-DHX (**5**)[d]	Full	0.5	0.49	10/3	0.4	0.47	3/1	0.0	0.49	71/22	0.0	0.44	57/24
3a*S*,9a*R*-(-)-**6a**[d]	Full	0.0	0.60	6/6	0.0	0.53	5/5	0.0	0.53	9/9	0.0	0.54	12/12
Quinpirole (**7**)[d]	Full	0.0	0.37	8/6	0.0	0.38	5/5	0.0	0.36	9/9	0.0	0.36	9/7
S-5-OH-DPAT (**8a**)	Full	1.2	0.61	82/17	1.7	0.57	78/21	1.2	0.55	130/29	2.1	0.57	140/30
R-3-PPP (**10a**)[d]	Full	3.1	0.67	34/2	3.5	0.68	26/3	3.2	0.70	68/6			43/0
Apomorphine (**11**)	Full	0.0	0.54	2/1	0.0	0.56	2/1	0.0	0.47	2/2	0.0	0.47	4/4
Dopamine (**12**)	Full	0.0	0.65	2/1	0.0	0.66	8/3	0.0	0.64	16/3	0.0	0.61	20/6
A70108 (**13a**)	Full	2.4	0.65	3/1	2.2	0.57	6/2	1.1	0.61	15/4	2.8	0.58	10/1
R-5-OH-DPAT (**8b**)	Partial			80/0			75/0	3.0	0.74	131/2			140/0
S-3-PPP[d] (**10b**)	Partial			34/0			18/0			68/0			54/0
S-6-OH-DPAT (**14**)	Partial	1.2	0.56	81/19	1.7	0.53	82/22	1.2	0.51	193/44	2.1	0.54	154 /34
R-7-OH-DPAT (**15a**)	Partial	1.2	0.57	81/17	1.8	0.65	84/16	1.2	0.62	193/37	2.1	0.63	152/28
S-Sumanirole (**3b**)	Inactive			5/1			5/0			5/0	1.5	0.62	3/1
SS-PHNO (**4b**)[d]	Inactive			9/0			6/0			22/0			16/0
3a*R*,9a*S*-(+)-**6b**[d]	Inactive			6/0			5/0			10/0			12/0
A70360 (**13b**)	Inactive			2/0			5/0			20/0			15/0
S-7-OH-DPAT (**15b**)	Inactive			82/0			79/0			189/0			151/0
cis-DHX (**16c**)	Inactive			2/0			6/0			11/0			12/0
(-)-DHX (**16b**)	Inactive			1/0			2/0			9/0			14/0
(+)-A86929 (**18a**)	Inactive			12/0			11/0	0.0	0.63	30/4	0.0	0.64	48/23
A77636 (**19a**)	Inactive			2/0			3/0			8/0			11/0
A77641 (**19b**)	Inactive			2/0			3/0			7/0			11/0
SKF-38393 (**20**)	Inactive	2.3	0.51	3/1			5/0			13/0			22/0

[a]The relative energy [kcal mol^{-1}] of the conformer that fit the pharmacophore model, related to the most stable conformer in the ensemble.[b] Root of the mean square distance between the center of the pharmacophore features and their matching ligand annotation points. [c]#c: number of conformations generated using the assigned method; #h: number of conformations that hit the pharmacophore model. [d] The tertiary amine is considered chiral, and two different configurations have been used in the modeling. [e]The energy cut-off for conformations generated in MOE is 4 kcal mol^{-1}. [f]The energy cut-off for conformations generated in Macromodel is 16.7 kJ mol^{-1} (approximately 4 kcal mol^{-1}).

Table A2. Results of the D_1 agonist pharmacophore search of four different ensembles of generated conformations.

Ligand		*MOE conformational import Born solvation, MMFF94(S)*[c]			*MOE stochastic search Born solvation, MMFF94(S)*[c]			*MacroModel serial torsion search GB/SA solvation, MMFF(S)*[f]			*MacroModel serial torsion search GB/SA solvation, OPLS2005*[f]		
		ΔE[a]	RMSD[b]	#c/#h[c]	ΔE[a]	RMSD[b]	#/#h[c]	ΔE[a]	RMSD[b]	#c/#h[c]	ΔE[a]	RMSD[b]	#c/#[c]
Dopamine (**12**)	Full	0	0.65	6/1	0	0.66	6/1	0	0.65	16/6	0	0.64	20/8
A70360 (**13b**)	Full			2/0	0	0.67	7/5	1.1	0.63	22/9	2.1	0.67	13/5
DHX (**16a**)	Full	0	0.17	1/1	0	0.23	2/1	0	0.15	9/5	0	0.13	14/8
Doxanthrine (**17**)	Full	0	0.14	1/1	0	0.12	2/2	0	0.13	7/3	0	0.11	14/6
(-)-A86929 (**18a**)	Full	0	0.48	12/12	0	0.54	10/10	0.3	0.14	33/14	0.5	0.12	73/36
A77636 (**19a**)	Full	1.2	0.25	2/1	0	0.28	3/2	0	0.23	8/4	0	0.26	11/7
SKF89626 (**21**)	Full	0	0.62	4/1	0.1	0.61	4/2	0	0.62	8/4	0	0.63	20/6
Zelandopam (**22**)	Full			4/0			4/0			13/0	2.9	0.63	40/2
SKF82958[d] (**23**)	Full	0	0.38	16/2	1.8	0.41	22/1	0	0.39	57/4	0	0.43	50/8
24a	Full	0	0.59	2/2	0	0.22	2/2	0	0.15	9/5	0	0.13	6/4
24b	Full	0	0.59	1/1	0	0.23	2/2	0	0.15	9/5	0	0.12	12/6
Dinapsoline (**25a**)	Full	0	0.36	2/1	0	0.39	1/1	0	0.36	3/2	0	0.45	6/4
Apomorphine (**11**)	Partial	0	0.62	2/1	0	0.61	2/1			2/0	0	0.62	4/2
A70108 (**13a**)	Partial			3/0	0.0	0.71	6/3	0.0	0.68	15/8	0.0	0.72	11/7
A77641 (**19b**)	Partial			2/0			3/0	3.6	0.65	8/1	2.8	0.67	11/2
SKF38393 (**20**)	Partial	0	0.66	3/3	0	0.43	5/3	0	0.45	12/8	0	0.62	20/10
24c	Partial			2/0			2/0			9/0			8/0
CY-208-243 (**27**)	Partial			2/0			3/0			3/0			1/0
R-NPA[d] (**1**)	Inactive			10/0			6/0			22/0			27/0
R-Sumanirole (**3a**)	Inactive			5/0			5/0			5/0			4/0
nPr-DHX[d] (**5**)	inactive			16/0			17/0			72/0			56/0
Quinpirole (**7**)	Inactive			8/0			4/0			8/0			9/0
(-)-DHX (**16b**)	inactive			1/0	0.8	0.74	2/1	0.4	0.75	11/2			8/0
cis-DHX (**16c**)	Inactive			2/0	2.7	0.62	5/1	1.9	0.61	11/4	3.4	0.62	12/4
(+)-A86929 **18b**	inactive			13/0			10/0	1.4	0.75	34/13			49/0
Ro 21-7767[d] (**28**)	Inactive			3/0			4/0			13/0			8/0
Rotigotine[d] (**29**)	inactive	2.5	0.66	232/2	3.6	0.69	186/2	3.4	0.69	375/2			486/0

[a]The relative energy [kcal mol^{-1}] of the conformer that fit the pharmacophore model, related to the most stable conformer in the ensemble.[b] Root of the mean square distance between the center of the pharmacophore features and their matching ligand annotation points. [c]#c: number of conformations generated using the assigned method; #h: number of conformations that hit the pharmacophore model. [d] The tertiary amine is considered chiral, and two different configurations have been used in the modeling. [e]The energy cut-off for conformations generated in MOE is 4 kcal mol^{-1}. [f]The energy cut-off for conformations generated in Macromodel is 16.7 kJ mol^{-1} (approximately 4 kcal mol^{-1}).

```
CLUSTAL 2.0.11 multiple sequence alignment


drd1_human      -MRTLNTSAMDG-----------TGLVVERDFSVRILTACFLSLLILSTLLGNTLVCAAV 48
drd2_human      -MDPLNLSWYDDDLERQNWSRPFNGSDGKADRPHYNYYATLLTLLIAVIVFGNVLVCMAV 59
adrb2_human     MGQPGNGSAFLLAPNRS--HAPDHDVTQQRDEVWVVGMGIVMSLIVLAIVFGNVLVITAI 58
                   . * *                .   : *       . .:::*::   ::**.**  *:

drd1_human      IRFRHLRSKVTNFFVISLAVSDLLVAVLVMPWKAVAEIAGFWPFG-SFCNIWVAFDIMCS 107
drd2_human      SREKALQT-TTNYLIVSLAVADLLVATLVMPWVVYLEVVGEWKFSRIHCDIFVTLDVMMC 118
adrb2_human     AKFERLQT-VTNYFITSLACADLVMGLAVVPFGAAHILMKMWTFGNFWCEFWTSIDVLCV 117
                 : . *:: .**::: *** :**::.  *:*: .   :   * *.   *:::.::*::

drd1_human      TASILNLCVISVDRYWAISSPFRYERKMTPK-AAFILISVAWTLSVLISFIPVQLSWHKA 166
drd2_human      TASILNLCAISIDRYTAVAMPMLYNTRYSSKRRVTVMISIVWVLSFTIS-CPLLFGLNNA 177
adrb2_human     TASIETLCVIAVDRYFAITSPFKYQSLLTKN-KARVIILMVWIVSGLTSFLPIQMHWYRA 176
                **** .**.*::*** *:: *: *:   : :  . ::* :.* :*   *  *: :   .*

drd1_human      KPTSPSDGNATSLAETIDNCDSSLSRTYAISSSVISFYIPVAIMIVTYTRIYRIAQKQIR 226
drd2_human      ------DQNECIIAN----------PAFVVYSSIVSFYVPFIVTLLVYIKIYIVLRRRR- 220
adrb2_human     T-----HQEAINCYANETCCDFFTNQAYAIASSIVSFYVPLVIMVFVYSRVFQEAKRQLQ 231
                      . :                  ::.: **::***:*. : :..* :::   :::

drd1_human      RIAALERAAVHAKNCQTTTGNGKPVECSQPESSFKMSFKRETKVLKTLSVIMGVFVCCWL 286
drd2_human      ------------------------------------SQQKEKKATQMLAIVLGVFIICWL 235
adrb2_human     KIDKSEGRFHVQNLSQVEQDGRTG----HGLRRSSKFCLKEHKALKTLGIIMGTFTLCWL 287
                                                    :* *. : *.:::*.*  ***

drd1_human      PFFILNCILPFCGSGETQPFCIDSNTFDVFVWFGWANSSLNPIIY-AFNADFRKAFSTLL 345
drd2_human      PFFITHILNIHCDCN------IPPVLYSAFTWLGYVNSAVNPIIYTTFNIEFRKAFLKIL 289
adrb2_human     PFFIVNIVHVIQDNL------IRKEVYILLNWIGYVNSGFNPLIY-CRSPDFRIAFQELL 340
                **** : :    .        *    :  : *:*:.**..**:**   . :** **  :*

drd1_human      GCYRLCPATNNAIETVSINNNGAAMFSSHHEPRGSISKECNLVYLIPHAVGSSEDLKKEE 405
drd2_human      HC---------------------------------------------------------- 291
adrb2_human     CLRRSSLKAYG--NGYSSNGNTGEQSGYHVEQEKENKLLCEDLPGTEDFVGHQGTVPSDN 398


drd1_human      AAGIARPLEKLSPALSVILDYDTDVSLEKIQPITQNGQHPT 446
drd2_human      ------------------------------------------
adrb2_human     IDSQGRNCSTNDSLL-------------------------- 413
```

Figure A1. The initial multiple sequence alignment between dopamine D_1 (drd1), D_2 (drd2) and the adrenergic β_2 receptors obtained from ClustalW.

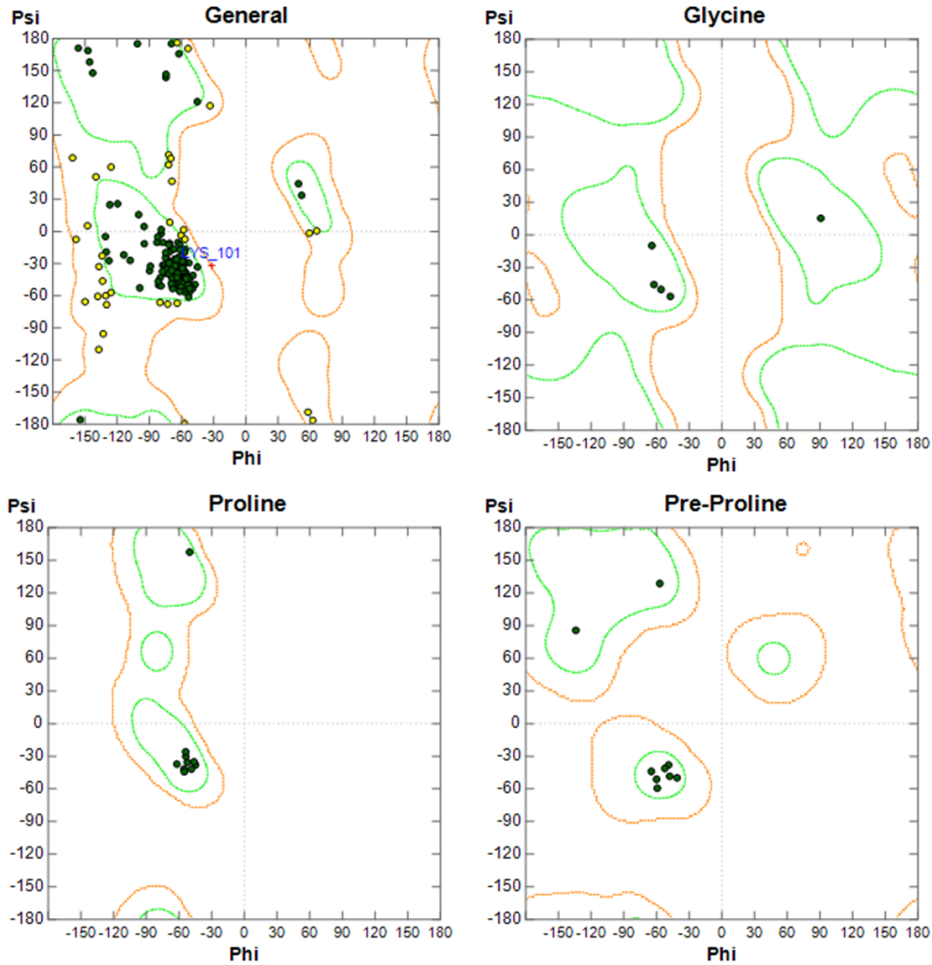

Figure A2. Ramachandran plots for glycines, prolin, pre-proline and for general residues of the selected dopamine D_2 homology model. The contours indicate allowed (orange) and core (green) regions of φ and Ψ angles, and the filled green rings indicate amino acids within the core regions while the yellow rings indicate allowed regions. A red cross indicates outliers. The outlier Lys101 1st extracellular loop (EC1) and the geometry are, therefore, considered to be acceptable.

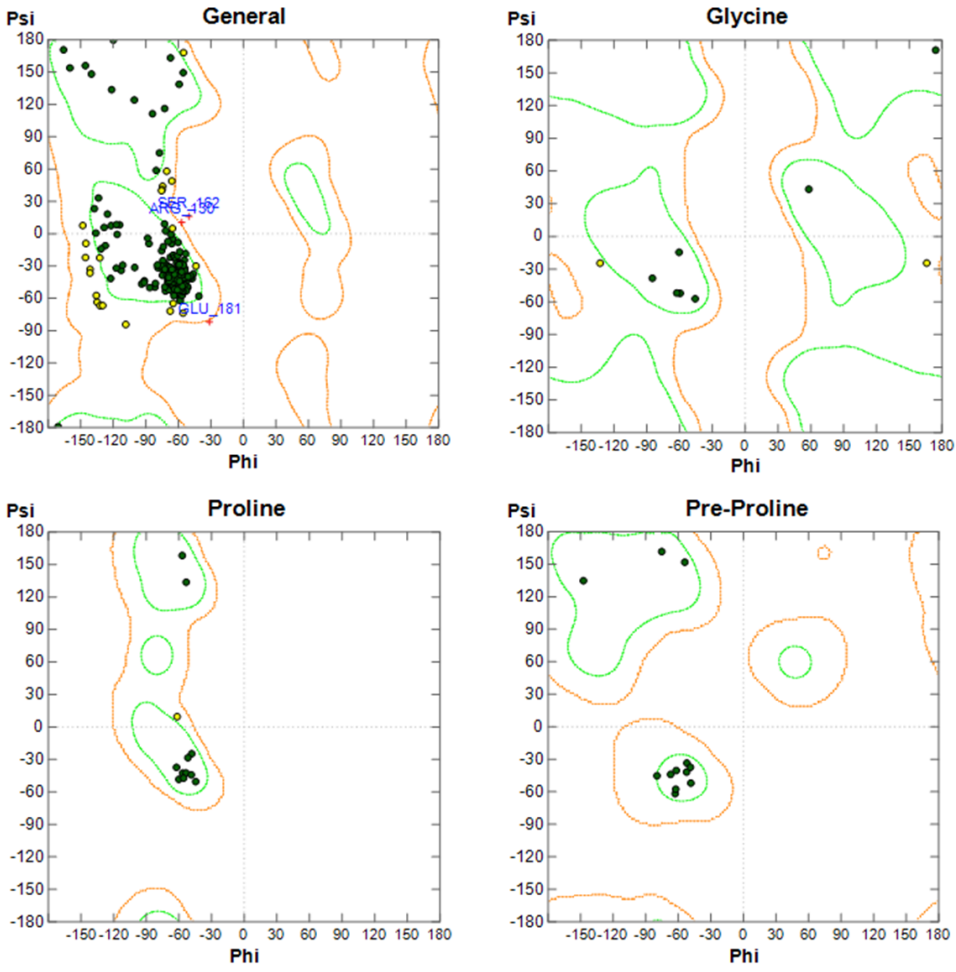

Figure A3. Ramachandran plots for glycines, prolines, pre-prolines and for general residues of the selected dopamine D_1 homology model. The contours indicate allowed (orange) and core (green) regions of φ and Ψ angles, and the filled green rings indicate amino acids within the core regions. The yellow rings indicate allowed regions. A red cross indicates outliers. The outliers Arg150, Ser162 and Glu181 are located in loops far apart from the binding site and are, therefore, considered to be acceptable.

9. References

1. Sousa, S. F.; Fernandes, P. A.; Ramos, M. J., Protein-ligand docking: current status and future challenges. *Proteins* **2006,** *65* (1), 15-26.

2. Berman, H. M.; Westbrook, J.; Feng, Z.; Gilliland, G.; Bhat, T. N.; Weissig, H.; Shindyalov, I. N.; Bourne, P. E., The Protein Data Bank. *Nucleic Acids Res.* **2000,** *28* (1), 235-242.

3. Cavasotto, C. N.; Phatak, S. S., Homology modeling in drug discovery: current trends and applications. *Drug Discov. Today* **2009,** *14* (13-14), 676-83.

4. Beaulieu, J. M.; Gainetdinov, R. R., The physiology, signaling, and pharmacology of dopamine receptors. *Pharmacol. Rev.* **2011,** *63* (1), 182-217.

5. Overington, J. P.; Al-Lazikani, B.; Hopkins, A. L., How many drug targets are there? *Nat. Rev. Drug Discov.* **2006,** *5* (12), 993-996.

6. Pauling, L.; Corey, R. B., Configurations of Polypeptide Chains with Favored Orientations around Single Bonds - 2 New Pleated Sheets. *Proc. Natl. Acad. Sci. U. S. A.* **1951,** *37* (11), 729-740.

7. Pauling, L.; Corey, R. B.; Branson, H. R., The Structure of Proteins - 2 Hydrogen-Bonded Helical Configurations of the Polypeptide Chain. *Proc. Natl. Acad. Sci. U. S. A.* **1951,** *37* (4), 205-211.

8. Thomson, A. J.; Gray, H. B., Bio-inorganic chemistry. *Curr. Opin. Chem. Biol.* **1998,** *2* (2), 155-8.

9. Freire, E., Do enthalpy and entropy distinguish first in class from best in class? *Drug Discov. Today* **2008,** *13* (19-20), 869-74.

10. Pauling, L., *Nature of the Chemical Bond.* Cornell University Press: 1960; p 88-107.

11. Moore, T. S.; Winmill, T. F., CLXXVII.-The state of amines in aqueous solution. *J. Chem. Soc. T.* **1912,** *101*, 1635-1676.

12. Arunan, E.; Desiraju, G. R.; Klein, R. A.; Sadlej, J.; Scheiner, S.; Alkorta, I.; Clary, D. C.; Crabtree, R. H.; Dannenberg, J. J.; Hobza, P.; Kjaergaard, H. G.; Legon, A. C.; Mennucci, B.; Nesbitt, D. J., Defining the hydrogen bond: An account (IUPAC Technical Report). *Pure Appl. Chem.* **2011,** *83* (8), 1619-1636.

13. Takahashi, O.; Kohno, Y.; Nishio, M., Relevance of weak hydrogen bonds in the conformation of organic compounds and bioconjugates: evidence from recent experimental data and high-level ab initio MO calculations. *Chem. Rev.* **2010,** *110* (10), 6049-76.

14. Baker, E. N.; Hubbard, R. E., Hydrogen bonding in globular proteins. *Prog. Biophys. Mol. Biol.* **1984,** *44* (2), 97-179.

15. Gilli, P.; Pretto, L.; Bertolasi, V.; Gilli, G., Predicting Hydrogen-Bond Strengths from Acid−Base Molecular Properties. The pKa Slide Rule: Toward the Solution of a Long-Lasting Problem. *Acc. Chem. Res.* **2008,** *42* (1), 33-44.

16. Tsuzuki, S.; Fujii, A., Nature and physical origin of CH/pi interaction: significant difference from conventional hydrogen bonds. *Phys. Chem. Chem. Phys.* **2008,** *10* (19), 2584-94.

17. Marsili, S.; Chelli, R.; Schettino, V.; Procacci, P., Thermodynamics of stacking interactions in proteins. *Phys. Chem. Chem. Phys.* **2008,** *10* (19), 2673-2685.

18. Headen, T. F.; Howard, C. A.; Skipper, N. T.; Wilkinson, M. A.; Bowron, D. T.; Soper, A. K., Structure of pi-pi interactions in aromatic liquids. *J. Am. Chem. Soc.* **2010,** *132* (16), 5735-42.

19. Lambert, D., Drugs and receptors. *CEACCP* **2004,** *4* (6), 181-184.

20. Strader, C. D.; Fong, T. M.; Tota, M. R.; Underwood, D.; Dixon, R. A., Structure and function of G protein-coupled receptors. *Annu. Rev. Biochem.* **1994,** *63*, 101-32.

21. Horn, F.; Bettler, E.; Oliveira, L.; Campagne, F.; Cohen, F. E.; Vriend, G., GPCRDB information system for G protein-coupled receptors. *Nucleic Acids Res.* **2003,** *31* (1), 294-7.

22. Kjelsberg, M. A.; Cotecchia, S.; Ostrowski, J.; Caron, M. G.; Lefkowitz, R. J., Constitutive activation of the alpha 1B-adrenergic receptor by all amino acid substitutions at a single site. Evidence for a region which constrains receptor activation. *J. Biol. Chem.* **1992,** *267* (3), 1430-1433.

23. Liggett, S. B.; Caron, M. G.; Lefkowitz, R. J.; Hnatowich, M., Coupling of a mutated form of the human beta 2-adrenergic receptor to Gi and Gs. Requirement for multiple cytoplasmic domains in the coupling process. *J. Biol. Chem.* **1991,** *266* (8), 4816-4821.

24. Gether, U.; Lin, S.; Ghanouni, P.; Ballesteros, J. A.; Weinstein, H.; Kobilka, B. K., Agonists induce conformational changes in transmembrane domains III and VI of the beta(2) adrenoceptor. *EMBO J.* **1997,** *16* (22), 6737-6747.

25. Jensen, A. D.; Guarnieri, F.; Rasmussen, S. G. F.; Asmar, F.; Ballesteros, J. A.; Gether, U., Agonist-induced conformational changes at the cytoplasmic side of transmembrane segment 6 in the beta(2) adrenergic receptor mapped by site-selective fluorescent labeling. *J. Biol. Chem.* **2001,** *276* (12), 9279-9290.

26. Bhattacharya, S.; Hall, S. E.; Vaidehi, N., Agonist-induced conformational changes in bovine rhodopsin: Insight into activation of G-protein-coupled receptors. *J. Mol. Biol.* **2008,** *382* (2), 539-555.

27. Kobilka, B. K.; Deupi, X., Conformational complexity of G-protein-coupled receptors. *Trends Pharmacol. Sci.* **2007,** *28* (8), 397-406.

28. Rosenbaum, D. M.; Zhang, C.; Lyons, J. A.; Holl, R.; Aragao, D.; Arlow, D. H.; Rasmussen, S. G. F.; Choi, H. J.; DeVree, B. T.; Sunahara, R. K.; Chae, P. S.; Gellman, S. H.; Dror, R. O.; Shaw, D. E.; Weis, W. I.; Caffrey, M.; Gmeiner, P.; Kobilka, B. K., Structure and function of an irreversible agonist-beta(2) adrenoceptor complex. *Nature* **2011,** *469* (7329), 236-U129.

29. Warne, T.; Moukhametzianov, R.; Baker, J. G.; Nehme, R.; Edwards, P. C.; Leslie, A. G. W.; Schertler, G. F. X.; Tate, C. G., The structural basis for agonist and partial agonist action on a beta(1)-adrenergic receptor. *Nature* **2011,** *469* (7329), 241-U134.

30. Rasmussen, S. G. F.; Choi, H. J.; Fung, J. J.; Pardon, E.; Casarosa, P.; Chae, P. S.; DeVree, B. T.; Rosenbaum, D. M.; Thian, F. S.; Kobilka, T. S.; Schnapp, A.; Konetzki, I.; Sunahara, R. K.; Gellman, S. H.; Pautsch, A.; Steyaert, J.; Weis, W. I.; Kobilka, B. K., Structure of a nanobody-stabilized active state of the beta(2) adrenoceptor. *Nature* **2011,** *469* (7329), 175-U59.

31. Strange, P. G., Signaling mechanisms of GPCR ligands. *Curr. Opin. Drug. Discov. Devel.* **2008,** *11* (2), 196-202.

32. Kenakin, T., Functional selectivity through protean and biased agonism: Who steers the ship? *Mol. Pharmacol.* **2007,** *72* (6), 1393-1401.

33. Kenakin, T., Being mindful of seven-transmembrane receptor 'guests' when assessing agonist selectivity. *Br. J. Pharmacol.* **2010,** *160* (5), 1045-1047.

34. Mary, S.; Damian, M.; Louet, M.; Floquet, N.; Fehrentz, J.-A.; Marie, J.; Martinez, J.; Banères, J.-L., Ligands and signaling proteins govern the conformational landscape explored by a G protein-coupled receptor. *Proc. Natl. Acad. Sci.* **2012,** *109* (21), 8304-8309.

35. Liu, W.; Chun, E.; Thompson, A. A.; Chubukov, P.; Xu, F.; Katritch, V.; Han, G. W.; Roth, C. B.; Heitman, L. H.; AP, I. J.; Cherezov, V.; Stevens, R. C., Structural basis for allosteric regulation of GPCRs by sodium ions. *Science* **2012,** *337* (6091), 232-6.

36. Horstman, D. A.; Brandon, S.; Wilson, A. L.; Guyer, C. A.; Cragoe, E. J., Jr.; Limbird, L. E., An aspartate conserved among G-protein receptors confers allosteric regulation of alpha 2-adrenergic receptors by sodium. *J. Biol. Chem.* **1990,** *265* (35), 21590-5.

37. Seeman, P.; Ulpian, C.; Grigoriadis, D.; Pribar, I.; Buchman, O., Conversion of Dopamine-D1 Receptors from High to Low Affinity for Dopamine. *Biochem. Pharmacol.* **1985,** *34* (1), 151-154.

38. Neve, K. A., Regulation of Dopamine D2 Receptors by Sodium and Ph. *Mol. Pharmacol.* **1991,** *39* (4), 570-578.

39. Makman, M. H.; Dvorkin, B.; Klein, P. N., Sodium-Ion Modulates D2 Receptor Characteristics of Dopamine Agonist and Antagonist Binding-Sites in Striatum and Retina. *Proc. Natl. Acad. Sci. U. S. A.-Biol. Sci.* **1982,** *79* (13), 4212-4216.

40. Ghanouni, P.; Schambye, H.; Seifert, R.; Lee, T. W.; Rasmussen, S. G. F.; Gether, U.; Kobilka, B. K., The effect of pH on beta(2) adrenoceptor function - Evidence for protonation-dependent activation. *J. Biol. Chem.* **2000,** *275* (5), 3121-3127.

41. Schetz, J. A., Allosteric modulation of dopamine receptors. *Mini-Rev. Med. Chem.* **2005,** *5* (6), 555-561.

42. Scheer, A.; Fanelli, F.; Costa, T.; DeBenedetti, P. G.; Cotecchia, S., Constitutively active mutants of the alpha(1B)-adrenergic receptor: Role of highly conserved polar amino acids in receptor activation. *EMBO J.* **1996,** *15* (14), 3566-3578.

43. Rasmussen, S. G. F.; Jensen, A. D.; Liapakis, G.; Ghanouni, P.; Javitch, J. A.; Gether, U., Mutation of a highly conserved aspartic acid in the beta(2) adrenergic receptor: Constitutive activation, structural instability, and conformational rearrangement of transmembrane segment 6. *Mol. Pharmacol.* **1999,** *56* (1), 175-184.

44. Ballesteros, J. A.; Weinstein, H., Integrated methods for the construction of three-dimensional models and computational probing of structure-function relations in G protein-coupled receptors. *Methods Neurosci.* **1995,** *25*, 366-428.

45. Palczewski, K.; Kumasaka, T.; Hori, T.; Behnke, C. A.; Motoshima, H.; Fox, B. A.; Le Trong, I.; Teller, D. C.; Okada, T.; Stenkamp, R. E.; Yamamoto, M.; Miyano, M., Crystal structure of rhodopsin: A G protein-coupled receptor. *Science* **2000,** *289* (5480), 739-45

46. Hibert, M. F.; Trumppkallmeyer, S.; Bruinvels, A.; Hoflack, J., 3-Dimensional Models of Neurotransmitter G-Binding Protein-Coupled Receptors. *Mol. Pharmacol.* **1991,** *40* (1), 8-15.

47. Mansour, A.; Meng, F.; Meador-Woodruff, J. H.; Taylor, L. P.; Civelli, O.; Akil, H., Site-Directed Mutagenesis of the Human Dopamine-D2 Receptor. *Eur. J. Pharmacol.* **1992,** *227* (2), 205-214.

48. Wiens, B. L.; Nelson, C. S.; Neve, K. A., Contribution of serine residues to constitutive and agonist induced signaling via the D-2S dopamine receptor: Evidence for multiple, agonist-specific active conformations. *Mol. Pharmacol.* **1998,** *54* (2), 435-444.

49. Coley, C.; Woodward, R.; Johansson, A. M.; Strange, P. G.; Naylor, L. H., Effect of multiple serine/alanine mutations in the transmembrane spanning region V of the D-2 dopamine receptor on ligand binding. *J. Neurochem.* **2000,** *74* (1), 358-366.

50. Cox, B. A.; Henningsen, R. A.; Spanoyannis, A.; Neve, R. L.; Neve, K. A., Contributions of Conserved Serine Residues to the Interactions of Ligands with Dopamine-D2 Receptors. *J. Neurochem.* **1992,** *59* (2), 627-635.

51. Cho, W.; Taylor, L. P.; Mansour, A.; Akil, H., Hydrophobic Residues of the D-2 Dopamine-Receptor Are Important for Binding and Signal-Transduction. *J. Neurochem.* **1995,** *65* (5), 2105-2115.

52. Tschammer, N.; Dorfler, M.; Hubner, H.; Gmeiner, P., Engineering a GPCR-Ligand Pair That Simulates the Activation of D-2L by Dopamine. *ACS Chem. Neurosci.* **2010,** *1* (1), 25-35.

53. Chen, S.; Xu, M.; Lin, F.; Lee, D.; Riek, P.; Graham, R. M., Phe310 in Transmembrane VI of the α1B-Adrenergic Receptor Is a Key Switch Residue Involved in Activation and Catecholamine Ring Aromatic Bonding. *J. Biol. Chem.* **1999,** *274* (23), 16320-16330.

54. Nyrönen, T.; Pihlavisto, M.; Peltonen, J. M.; Hoffrén, A.-M.; Varis, M.; Salminen, T.; Wurster, S.; Marjamäki, A.; Kanerva, L.; Katainen, E.; Laaksonen, L.; Savola, J.-M.; Scheinin, M.; Johnson, M. S., Molecular Mechanism for Agonist-Promoted α_{2A}-Adrenoceptor Activation by Norepinephrine and Epinephrine. *Mol. Pharmacol.* **2001,** *59* (5), 1343-1354.

55. Carlsson, A.; Lindqvist, M.; Magnusson, T., 3,4-Dihydroxyphenylalanine and 5-hydroxytryptophan as reserpine antagonists. *Nature* **1957,** *180* (4596), 1200.

56. Jackson, D. M.; Westlind-Danielsson, A., Dopamine-Receptors - Molecular-Biology, Biochemistry and Behavioral-Aspects. *Pharmacol. Ther.* **1994,** *64* (2), 291-370.

57. Goldman, M. E.; Kebabian, J. W., Aporphine Enantiomers - Interactions with D-1 and D-2 Dopamine-Receptors. *Mol. Pharmacol.* **1984,** *25* (1), 18-23.

58. Thobois, S., Proposed dose equivalence for rapid switch between dopamine receptor agonists in Parkinson's disease: A review of the literature. *Clin. Ther.* **2006,** *28* (1), 1-12.

59. Goldstein, M.; Lew, J. Y.; Nakamura, S.; Battista, A. F.; Lieberman, A.; Fuxe, K., Dopaminephilic properties of ergot alkaloids. *Fed. Proc.* **1978,** *37* (8), 2202-6.

60. Bedard, P. J.; Boucher, R., Effect of D1-Receptor Stimulation in Normal and Mptp Monkeys. *Neurosci. Lett.* **1989,** *104* (1-2), 223-228.

61. Emre, M.; Rinne, U. K.; Rascol, A.; Lees, A.; Agid, Y.; Lataste, X., Effects of a Selective Partial D1 Agonist, Cy 208-243, in Denovo Patients with Parkinson Disease. *Mov. Disord.* **1992,** *7* (3), 239-243.

62. Rascol, O.; Nutt, J. G.; Blin, O.; Goetz, C. G.; Trugman, J. M.; Soubrouillard, C.; Carter, J. H.; Currie, L. J.; Fabre, N.; Thalamas, C.; Giardina, W. J.; Wright, S., Induction by dopamine D-1 receptor agonist ABT-431 of dyskinesia similar to levodopa in patients with Parkinson disease. *Arch. Neurol.* **2001,** *58* (2), 249-254.

63. Blanchet, P. J.; Fang, J.; Gillespie, M.; Sabounjian, L. A.; Locke, K. W.; Gammans, R.; Mouradian, M. M.; Chase, T. N., Effects of the full dopamine D1 receptor agonist dihydrexidine in Parkinson's disease. *Clin. Neuropharmacol.* **1998,** *21* (6), 339-343.

64. Burkert, U. A., N. L. , *Molecular Mechanics.* ACS Monograph 177, American Chemical Society: Washington, D.C., 1982.

65. Cornell, W. D.; Cieplak, P.; Bayly, C. I.; Gould, I. R.; Merz, K. M.; Ferguson, D. M.; Spellmeyer, D. C.; Fox, T.; Caldwell, J. W.; Kollman, P. A., A 2nd Generation Force-Field for the Simulation of Proteins, Nucleic-Acids, and Organic-Molecules. *J. Am. Chem. Soc.* **1995,** *117* (19), 5179-5197.

66. Jorgensen, W. L.; Tirado-Rives, J., The OPLS [optimized potentials for liquid simulations] potential functions for proteins, energy minimizations for crystals of cyclic peptides and crambin. *J. Am. Chem. Soc.* **1988,** *110* (6), 1657-1666.

67. Jorgensen, W. L.; Maxwell, D. S.; Tirado-Rives, J., Development and Testing of the OPLS All-Atom Force Field on Conformational Energetics and Properties of Organic Liquids. *J. Am. Chem. Soc.* **1996,** *118* (45), 11225-11236.

68. Halgren, T. A., Merck molecular force field. I. Basis, form, scope, parameterization, and performance of MMFF94. *J. Comput. Chem.* **1996,** *17* (5-6), 490-519.

69. Halgren, T. A., MMFF VI. MMFF94s option for energy minimization studies. *J. Comput. Chem.* **1999,** *20* (7), 720-729 and 730-748.

70. Banks, J. L.; Beard, H. S.; Cao, Y.; Cho, A. E.; Damm, W.; Farid, R.; Felts, A. K.; Halgren, T. A.; Mainz, D. T.; Maple, J. R.; Murphy, R.; Philipp, D. M.; Repasky, M. P.; Zhang, L. Y.; Berne, B. J.; Friesner, R. A.; Gallicchio, E.; Levy, R. M., Integrated Modeling Program, Applied Chemical Theory (IMPACT). *J. Comput. Chem.* **2005,** *26* (16), 1752-1780.

71. Still, W. C.; Tempczyk, A.; Hawley, R. C.; Hendrickson, T., Semianalytical treatment of solvation for molecular mechanics and dynamics. *J. Am. Chem. Soc.* **1990,** *112* (16), 6127-6129.

72. Wojciechowski, M.; Lesyng, B., Generalized Born Model: Analysis, Refinement, and Applications to Proteins. *J. Phys. Chem. B* **2004,** *108* (47), 18368-18376.

73. Kolossavary, I.; Guida, W. C., Low-mode conformational search elucidated: Application to C39H80 and flexible docking of 9-deazaguanine inhibitors into PNP. *J. Comput. Chem.* **1999,** *20* (15), 1671-1684.

74. Kolossvary, I.; Guida, W. C., Low mode search. An efficient, automated computational method for conformational analysis: Application to cyclic and acyclic alkanes and cyclic peptides. *J. Am. Chem. Soc.* **1996,** *118* (21), 5011-5019.

75. Kirkpatrick, S.; Gelatt, C. D., Jr.; Vecchi, M. P., Optimization by simulated annealing. *Science* **1983,** *220* (4598), 671-80.

76. Ferguson, D. M.; Raber, D. J., A new approach to probing conformational space with molecular mechanics: random incremental pulse search. *J. Am. Chem. Soc.* **1989,** *111* (12), 4371-4378.

77. Nicholas, M.; Arianna, W. R.; Marshall, N. R.; Augusta, H. T.; Edward, T., Equation of State Calculations by Fast Computing Machines. *J. Chem. Phys.* **1953,** *21* (6), 1087-1092.

78. Kaczanowski, S.; Zielenkiewicz, P., Why similar protein sequences encode similar three-dimensional structures? *Theor. Chem. Acc.* **2010,** 125(3), 643-650.

79. Sali, A.; Blundell, T. L., Comparative protein modelling by satisfaction of spatial restraints. *J. Mol. Biol.* **1993,** *234* (3), 779-815.

80. MacroModel version 9.5; Schrodinger, LLC: **2007**.

81. Arnold, K.; Bordoli, L.; Kopp, J.; Schwede, T., The SWISS-MODEL workspace: a web-based environment for protein structure homology modelling. *Bioinformatics* **2006,** *22* (2), 195-201.

82. ICM version 3.4; Molsoft LLC: San Diego, CA, USA, **2005**.

83. MOE version 2005.06, 2007.0902, 2009.10; Chemical Computing Group Inc.: Montreal.

84. Labute, P., Protonate3D: Assignment of ionization states and hydrogen coordinates to macromolecular structures. *Proteins: Struct., Funct., Bioinf.* **2009,** *75* (1), 187-205.

85. Laskowski, R. A.; Macarthur, M. W.; Moss, D. S.; Thornton, J. M., Procheck - a Program to Check the Stereochemical Quality of Protein Structures. *J. Appl. Crystallogr.* **1993,** *26*, 283-291.

86. Bostrom, J.; Norrby, P. O.; Liljefors, T., Conformational energy penalties of protein-bound ligands. *J. Comput. Aided Mol. Des.* **1998,** *12* (4), 383-396.

87. CATALYST MolecularSimulations Inc.: San Diego, CA, USA.

88. Brooks, B. R.; Bruccoleri, R. E.; Olafson, B. D.; States, D. J.; Swaminathan, S.; Karplus, M., CHARMM: A program for macromolecular energy, minimization, and dynamics calculations. *J. Comput. Chem.* **1983,** *4* (2), 187-217.

89. Smellie, A.; Teig, S. L.; Towbin, P., Poling: Promoting conformational variation. *J. Comput. Chem.* **1995,** *16* (2), 171-187.

90. Dixon, S. L.; Smondyrev, A. M.; Knoll, E. H.; Rao, S. N.; Shaw, D. E.; Friesner, R. A., PHASE: a new engine for pharmacophore perception, 3D QSAR model development, and 3D database screening: 1. Methodology and preliminary results. *J. Comput. Aided Mol. Des.* **2006,** *20* (10-11), 647-71.

91. Wolber, G.; Langer, T., LigandScout: 3-D pharmacophores derived from protein-bound ligands and their use as virtual screening filters. *J. Chem. Inf. Model* **2005,** *45* (1), 160-9.

92. Tschammer, N.; Bollinger, S.; Kenakin, T.; Gmeiner, P., Histidine 6.55 is a major determinant of ligand biased signaling in dopamine D2L receptor. *Mol. Pharmacol.* **2011,** *79* (3), 575-585.

93. Shi, L.; Javitch, J. A., The second extracellular loop of the dopamine D-2 receptor lines the binding-site crevice. *Proc. Natl. Acad. Sci. U. S. A.* **2004,** *101* (2), 440-445.

94. Zeng, F. Y.; Soldner, A.; Schoneberg, T.; Wess, J., Conserved extracellular cysteine pair in the M-3 muscarinic acetylcholine receptor is essential for proper receptor cell surface localization but not for G protein coupling. *J. Neurochem.* **1999,** *72* (6), 2404-2414.

95. Noda, K.; Saad, Y.; Graham, R. M.; Karnik, S. S., The High-Affinity State of the Beta-2-Adrenergic Receptor Requires Unique Interaction between Conserved and Nonconserved Extracellular Loop Cysteines. *J. Biol. Chem.* **1994,** *269* (9), 6743-6752.

96. Cannon, J. G., Structure-activity relationships of dopamine agonists. *Annu. Rev. Pharmacol. Toxicol.* **1983,** *23*, 103-29.

97. Pettersson, I.; Liljefors, T., Structure-activity relationships for apomorphine congeners. Conformational energies vs. biological activities. *J. Comput. Aided Mol. Des.* **1987,** *1* (2), 143-152.

98. Tonani, R.; Dunbar, J., Jr.; Edmonston, B.; Marshall, G. R., Computer-aided molecular modeling of a D2-agonist dopamine pharmacophore. *J. Comput. Aided Mol. Des.* **1987,** *1* (2), 121-32.

99. Johansson, A. M.; Grol, C. J.; Karlen, A.; Hacksell, U., Dopamine D2 receptor agonists: an analysis of indirect models. *Drug Des. Discov.* **1994,** *11* (2), 159-74.

100. Wikstrom, H., Centrally acting dopamine D2 receptor ligands: agonists. *Prog. Med. Chem.* **1992,** *29*, 185-216.

101. Seeman, P.; Watanabe, M.; Grigoriadis, D.; Tedesco, J. L.; George, S. R.; Svensson, U.; Nilsson, J. L.; Neumeyer, J. L., Dopamine D2 receptor binding sites for agonists. A tetrahedral model. *Mol. Pharmacol.* **1985,** *28* (5), 391-9.

102. Parrish, J. C.; Braden, M. R.; Gundy, E.; Nichols, D. E., Differential phospholipase C activation by phenylalkylamine serotonin 5-HT 2A receptor agonists. *J. Neurochem.* **2005,** *95* (6), 1575-84.

103. Anden, N. E.; Nilsson, H.; Ros, E.; Thornstrom, U., Effects of B-HT 920 and B-HT 933 on dopamine and noradrenaline autoreceptors in the rat brain. *Acta Pharmacol. Toxicol. (Copenh).* **1983,** *52* (1), 51-6.

104. Eriksson, E.; Svensson, K.; Clark, D., The putative dopamine autoreceptor agonist B-HT 920 decreases nigral dopamine cell firing rate and prolactin release in rat. *Life Sci.* **1985,** *36* (19), 1819-27.

105. Kearsley, S. K.; Smith, G. M., An alternative method for the alignment of molecular structures: maximizing electrostatic and steric overlap. *Tetrahedron Comput. Meth.* **1990,** *3* (6c), 615-33.

106. Bondi, A., Van Der Waals Volumes + Radii. *J. Phys. Chem.* **1964,** *68* (3), 441-&.

107. Liljefors, T.; Wikstrom, H., A Molecular Mechanics Approach to the Understanding of Presynaptic Selectivity for Centrally Acting Dopamine Receptor Agonists of the Phenylpiperidine Series. *J. Med. Chem.* **1986,** *29* (10), 1896-1904.

108. Yarov-Yarovoy, V.; Schonbrun, J.; Baker, D., Multipass membrane protein structure prediction using Rosetta. *Proteins* **2006,** *62* (4), 1010-25.

109. Shacham, S.; Marantz, Y.; Bar-Haim, S.; Kalid, O.; Warshaviak, D.; Avisar, N.; Inbal, B.; Heifetz, A.; Fichman, M.; Topf, M.; Naor, Z.; Noiman, S.; Becker, O. M., PREDICT modeling and in-silico screening for G-protein coupled receptors. *Proteins* **2004,** *57* (1), 51-86.

110. Vaidehi, N.; Floriano, W. B.; Trabanino, R.; Hall, S. E.; Freddolino, P.; Choi, E. J.; Zamanakos, G.; Goddard, W. A., 3rd, Prediction of structure and function of G protein-coupled receptors. *Proc. Natl. Acad. Sci. U. S. A.* **2002,** *99* (20), 12622-7.

111. Kalani, M. Y.; Vaidehi, N.; Hall, S. E.; Trabanino, R. J.; Freddolino, P. L.; Kalani, M. A.; Floriano, W. B.; Kam, V. W.; Goddard, W. A., 3rd, The predicted 3D structure of the human D2 dopamine receptor and the binding site and binding affinities for agonists and antagonists. *Proc. Natl. Acad. Sci. U. S. A.* **2004,** *101* (11), 3815-20.

112. Evers, A.; Klebe, G., Ligand-supported homology modeling of g-protein-coupled receptor sites: models sufficient for successful virtual screening. *Angew. Chem. Int. Ed. Engl.* **2004,** *43* (2), 248-51.

113. Chien, E. Y. T.; Liu, W.; Zhao, Q. A.; Katritch, V.; Han, G. W.; Hanson, M. A.; Shi, L.; Newman, A. H.; Javitch, J. A.; Cherezov, V.; Stevens, R. C., Structure of the Human Dopamine D3 Receptor in Complex with a D2/D3 Selective Antagonist. *Science* **2010,** *330* (6007), 1091-1095.

114. Jaakola, V. P.; Griffith, M. T.; Hanson, M. A.; Cherezov, V.; Chien, E. Y. T.; Lane, J. R.; IJzerman, A. P.; Stevens, R. C., The 2.6 Angstrom Crystal Structure of a Human A(2A) Adenosine Receptor Bound to an Antagonist. *Science* **2008,** *322* (5905), 1211-1217.

115. Cherezov, V.; Rosenbaum, D. M.; Hanson, M. A.; Rasmussen, S. G. F.; Thian, F. S.; Kobilka, T. S.; Choi, H. J.; Kuhn, P.; Weis, W. I.; Kobilka, B. K.; Stevens, R. C., High-resolution crystal structure of an engineered human beta(2)-adrenergic G protein-coupled receptor. *Science* **2007,** *318* (5854), 1258-1265.

116. Park, J. H.; Scheerer, P.; Hofmann, K. P.; Choe, H. W.; Ernst, O. P., Crystal structure of the ligand-free G-protein-coupled receptor opsin. *Nature* **2008,** *454* (7201), 183-U33.

117. Scheerer, P.; Park, J. H.; Hildebrand, P. W.; Kim, Y. J.; Krauss, N.; Choe, H. W.; Hofmann, K. P.; Ernst, O. P., Crystal structure of opsin in its G-protein-interacting conformation. *Nature* **2008,** *455* (7212), 497-U30.

118. Lebon, G.; Warne, T.; Edwards, P. C.; Bennett, K.; Langmead, C. J.; Leslie, A. G.; Tate, C. G., Agonist-bound adenosine A2A receptor structures reveal common features of GPCR activation. *Nature* **2011,** *474* (7352), 521-5.

119. Abagyan, R.; Totrov, M., Biased probability Monte Carlo conformational searches and electrostatic calculations for peptides and proteins. *J. Mol. Biol.* **1994,** *235* (3), 983-1002.

120. Okada, T.; Sugihara, M.; Bondar, A.-N.; Elstner, M.; Entel, P.; Buss, V., The Retinal Conformation and its Environment in Rhodopsin in Light of a New 2.2 Å Crystal Structure. *J. Mol. Biol.* **2004,** *342* (2), 571-583.

121. Carlsson, J.; Coleman, R. G.; Setola, V.; Irwin, J. J.; Fan, H.; Schlessinger, A.; Sali, A.; Roth, B. L.; Shoichet, B. K., Ligand discovery from a dopamine D3 receptor homology model and crystal structure. *Nat. Chem. Biol.* **2011,** *7* (11), 769-78.

122. Thompson, J. D.; Higgins, D. G.; Gibson, T. J., Clustal-W - Improving the Sensitivity of Progressive Multiple Sequence Alignment through Sequence Weighting, Position-Specific Gap Penalties and Weight Matrix Choice. *Nucleic Acids Res.* **1994,** *22* (22), 4673-4680.

123. Peeters, M. C.; van Westen, G. J. P.; Li, Q.; Ijzerman, A. P., Importance of the extracellular loops in G protein-coupled receptors for ligand recognition and receptor activation. *Trends Pharmacol. Sci.* **2011,** *32* (1), 35-42.

124. Wang, J. M.; Cieplak, P.; Kollman, P. A., How well does a restrained electrostatic potential (RESP) model perform in calculating conformational energies of organic and biological molecules? *J. Comput. Chem.* **2000,** *21* (12), 1049-1074.

125. Gao, Y. G.; Baldessarini, R. J.; Kula, N. S.; Neumeyer, J. L., Synthesis and Dopamine Receptor Affinities of Enantiomers of 2-Substituted Apomorphines and Their N-N-Propyl Analogs. *J. Med. Chem.* **1990,** *33* (6), 1800-1805.

126. Mottola, D. M.; Laiter, S.; Watts, V. J.; Tropsha, A.; Wyrick, S. D.; Nichols, D. E.; Mailman, R. B., Conformational analysis of D1 dopamine receptor agonists: pharmacophore assessment and receptor mapping. *J. Med. Chem.* **1996,** *39* (1), 285-96.

127. Chemel, B. R.; Bonner, L. A.; Watts, V. J.; Nichols, D. E., Ligand-specific roles for transmembrane 5 serine residues in the binding and efficacy of dopamine D(1) receptor catechol agonists. *Mol. Pharmacol.* **2012,** *81* (5), 729-38.

128. Pollock, N. J.; Manelli, A. M.; Hutchins, C. W.; Steffey, M. E.; Mackenzie, R. G.; Frail, D. E., Serine Mutations in Transmembrane-V of the Dopamine D1-Receptor Affect Ligand Interactions and Receptor Activation. *J. Biol. Chem.* **1992,** *267* (25), 17780-17786.

129. Deninno, M. P.; Schoenleber, R.; Asin, K. E.; Mackenzie, R.; Kebabian, J. W., (1*R*,3*S*)-1-(Aminomethyl)-3,4-dihydro-5,6-dihydroxy-3-phenyl-1*H*-2-benzopyran: A Potent and Selective D1 Agonist. *J. Med. Chem.* **1990,** *33* (11), 2948-2950.

130. Ryman-Rasmussen, J. P.; Nichols, D. E.; Mailman, R. B., Differential activation of adenylate cyclase and receptor internalization by novel dopamine D-1 receptor agonists. *Mol. Pharmacol.* **2005,** *68* (4), 1039-1048.

131. Erdelyi, M., Halogen bonding in solution. *Chem. Soc. Rev.* **2012,** *41* (9), 3547-57.

132. Cueva, J. P.; Giorgioni, G.; Grubbs, R. A.; Chemel, B. R.; Watts, V. J.; Nichols, D. E., trans-2,3-dihydroxy-6a,7,8,12b-tetrahydro-6H-chromeno[3,4-*c*]isoquinoline: Synthesis, resolution, and preliminary pharmacological characterization of a new dopamine D-1 receptor full agonist. *J. Med. Chem.* **2006,** *49* (23), 6848-6857.

133. Mottola, D. M.; Brewster, W. K.; Cook, L. L.; Nichols, D. E.; Mailman, R. B., Dihydrexidine, a Novel Full Efficacy D1-Dopamine Receptor Agonist. *J. Pharmacol. Exp. Ther.* **1992,** *262* (1), 383-393.

134. Andersen, P. H.; Nielsen, E. B.; Scheelkruger, J.; Jansen, J. A.; Hohlweg, R., Thienopyridine Derivatives Identified as the 1st Selective, Full Efficacy, Dopamine D1 Receptor Agonists. *Eur. J. Pharmacol.* **1987,** *137* (2-3), 291-292.

135. Ofori, S.; Deraad, S.; Bugnon, O.; Schorderet, M., Effects of YM-435 and A-77636 on Dopamine D-1 Receptors in Bovine Retina in-Vitro. *Gen. Pharmacol.* **1995,** *26* (1), 51-57.

136. Tomic, M.; Seeman, P.; George, S. R.; Odowd, B. F., Dopamine D1 Receptor Mutagenesis: Role of Amino Acids in Agonist and Antagonist Binding. *Biochem. Biophys. Res. Commun.* **1993,** *191* (3), 1020-1027.

137. Almaula, N.; Ebersole, B. J.; Zhang, D.; Weinstein, H.; Sealfon, S. C., Mapping the Binding Site Pocket of the Serotonin 5-Hydroxytryptamine2A Receptor. *J. Biol. Chem.* **1996,** *271* (25), 14672-14675.

138. Gu, Y. G.; Bayburt, E. K.; Michaelides, M. R.; Lin, C. W.; Shiosaki, K., trans-2,6-, 3,6-and 4,6-diaza-5,6,6a,7,8,12b-hexahydrobenzo[*c*]phenanthrene-10,11-diols as dopamine agonists. *Bioorg. Med. Chem. Lett.* **1999,** *9* (10), 1341-1346.

139. Sit, S. Y.; Xie, K.; Jacutin-Porte, S.; Boy, K. M.; Seanz, J.; Taber, M. T.; Gulwadi, A. G.; Korpinen, C. D.; Burris, K. D.; Molski, T. F.; Ryan, E.; Xu, C.; Verdoorn, T.; Johnson, G.; Nichols, D. E.; Mailman, R. B., Synthesis and SAR exploration of dinapsoline analogues. *Bioorg. Med. Chem.* **2004,** *12* (4), 715-734.

140. Wieland, K.; Zuurmond, H. M.; Krasel, C.; Ijzerman, A. P.; Lohse, M. J., Involvement of Asn-293 in stereospecific agonist recognition and in activation of the beta(2)-adrenergic receptor. *Proc. Natl. Acad. Sci. U. S. A.* **1996,** *93* (17), 9276-9281.